A COBALT OXIDE CARBON NANOTUBE COMPOSITE FOR DOPAMINE DETECTION

by

Mohammad Salauddin Kader

A Thesis Submitted in Partial Fulfillment of the Requirements for the Degree of

Master of Science in Chemistry

Middle Tennessee State University

August 2018

Thesis Committee:

Dr. Charles C. Chusuei, Major Professor

Dr. Chengshan Wang

Dr. Ngee-Sing Chong

ABSTRACT

Dopamine (DA) is a catecholamine and performs as a neurotransmitter in the human body. Dopamine plays an important role in the process of many biological networks. Research showed that unusual amounts of DA can cause several neurological diseases such as Parkinson's disease, schizophrenia and other mental disorder. Cobalt oxide (CoO) particles were tethered to carboxylic-acid-functionalized multi-walled carbon nanotubes (COOH-MWNT) using sonication. The resulting composite (CoO/COOH-MWNT) was applied to glassy carbon electrodes for detecting DA within the 0.5-5 μM range and 10-100 μM range. Current versus concentration was measured using cyclic voltammetry. Different parameters such as loading, pH and sonication times (0 to 60 min) were varied to optimize current response. Good selectivity was found against uric acid and ascorbic acid. The (CoO/COOH-MWNT) composite was characterized by attenuated total reflection infrared spectroscopy (ATR-IR), Raman spectroscopy, Transmission electron microscopy (TEM) and X-ray photoelectron spectroscopy (XPS).

TABLE OF CONTENTS

Page

LIST OF FIGURES

Page

LIST OF TABLES

Page

LIST OF SCHEMES

Page

CHAPTER I

INTRODUCTION

Nanomaterials occur naturally and can also be manufactured by engineering. Engineered nanomaterials (ENMs) are designed to get the advantage of their small size and unique properties. Nanomaterials are defined as a set of materials which have at least one dimension that is less than approximately 100 nm. Nanomaterials are approximately 100000 times smaller than human hair.[1,2] The interest of engineered nanomaterials due to their novel electrical, magnetic and optical properties. These properties of engineered nanomaterials have significant importance in medicine, electronics and other fields.[3] They can be also used in biosensors, medical diagnosis, drug delivery and environmental remediation. Engineered nanomaterials (ENMs) can be manufactured from minerals, metals, carbon and other chemical substance. The properties of the nanomaterials can vary depending on their particle size, shape, surface area, composition, and strength of particle bonds. Nanocrystals, dendrimers and carbon nanotubes are few examples of engineered nanomaterials (ENMs). Nanocrystals are composed of a quantum dot surrounded by semiconductor materials. Quantum dots are semiconductor materials in nanoscale level.[4] They showed unique properties in nano-sized structure. Dendrimers are monodispersed, radially symmetric, homogeneous nano-sized materials[5] and carbon nanotubes are allotropes of carbon in the form of a cylindrical structure.[6]

Carbon nanotube (CNT)

Carbon nanotubes (CNTs) are allotropes of carbon which have cylindrical structures.[6] Carbon nanotubes have unique properties which are important in the fields (biosensors, optics, electronics, etc.) of nanotechnology and materials science. There are mainly three methods to synthesis carbon nanotubes. Chemical vapor decomposition (CVD), arc-discharge and laser ablation (LA) methods are used to synthesis carbon nanotubes. During arc-discharge process, graphite rods are used to synthesis carbon nanotubes. Graphite rods produce arc during the process. These graphite rods also act as cathode and anode electrode. In the chemical vapor decomposition (CVD) process, carbon nanotubes accumulate on the metal catalysts. Metal catalysts decompose the gas, which is consist of carbon. The process is called catalytic decomposition. During laser ablation (LA) process, laser vaporized carbon/metal mixtures are used to produce carbon nanotubes. Caron/ metal mixture vaporization is done using laser beam then condensed the vaporized mixture to get the carbon nanotubes. Generally, chemical vapor decomposition (CVD) process is used to produce large scale of multi-walled carbon nanotubes (MWNTs). The process is inexpensive and uncomplicated. The CVD process is done at 500 to 1000°C temperature. On the other hand, single-walled carbon nanotubes (SWNTs) are extensively produced using laser ablation (LA) and arc-discharge process. These two processes are done at around 1200°C temperature, which is supportive for single-walled carbon nanotubes (SWNTs) formation.[7,8]

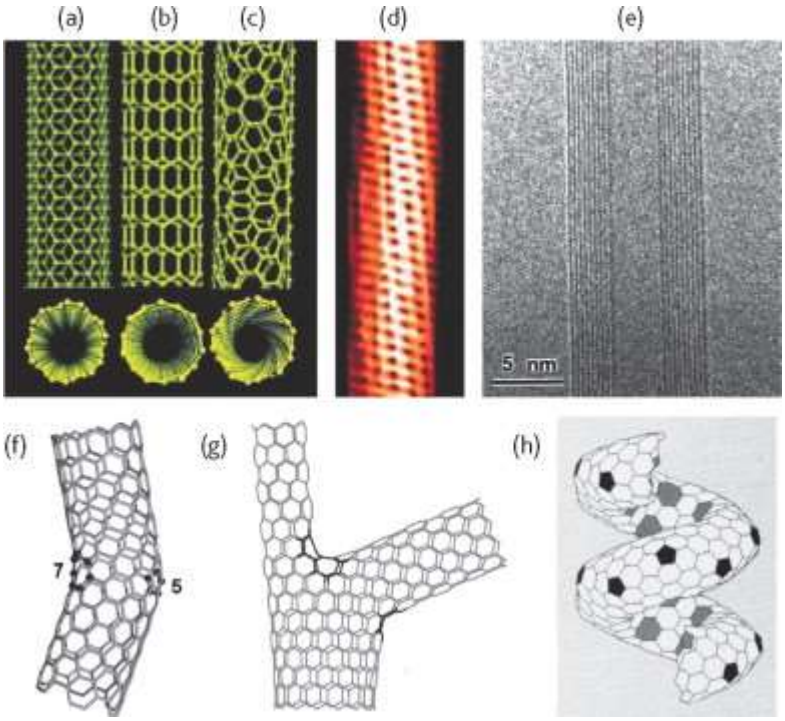

Figure 1: Different shape of carbon nanotube cylindrical structures. a) armchair, b) zigzag, c) chiral SWNT, d) SPM picture of 1.3 nm diameter chiral SWNT, e) TEM image of MWNT, f) kink junction in carbon bone, g) asymmetric SWNT structure, h) the helically coiled SWNT. (Figure reproduced with permission from reference 9).

Properties of carbon nanotube (CNT)

Carbon nanotubes (CNTs) have unique electrical, mechanical, and chemical properties which are important in material science and nanotechnology. Carbon nanotubes are promising materials for biosensors, drug delivery and tiny machines. CNTs shows extraordinarily high thermal conductivity. Due to the high thermal conductivity they are very efficient in conducting electricity. CNTs are better thermal conductor than diamonds. They have twice better thermal conductivity than diamonds. Their extraordinary electrical, structural and mechanical properties make them potential material in the field of nanoscience and technology. They are thermally stable up to 2800ºC. CNTs exhibit incredible tensile strength (tensile strength is the unit of energy to break any material) and elastic modulus (elastic modulus is the unit of material resistance).[10] CNTs have capacity to conduct electricity 1000 times higher than copper. CNTs can be conducting or semiconducting materials based on their structure. They have also big surface area and capability to modify other material surfaces. CNTs have very sharp tips which enable them to focus electric field and emit electrons at very low voltage. They can discharge electrons from the surface very easily. Due to these extraordinary properties, scientists are using carbon nanotubes in composite materials to modify characteristics of other materials. CNTs can perform in cellular level. They can target cancer cells and nerve cells. CNTs also perform as a promising material in drug delivery.[11] CNTs are used in the nanofiber to provide greater strength on their structure. Now a day, researches are aimed to solve problem in the field of nano-engineering, material science, biomedical, biosensors, and drug delivery using CNT's extraordinary properties.

Types of carbon nanotube (CNT)

According to the number of graphic shells, carbon nanotubes are mainly two types. a) Single-walled (SWNTs) and b) multi-walled carbon nanotubes (MWNTs). Several single-walled carbon nanotubes (SWNTs) group together and forms multi-walled carbon nanotubes (MWNTs). Single-walled carbon nanotubes (SWNTs) held together by van der Waals forces force and π-stacking.

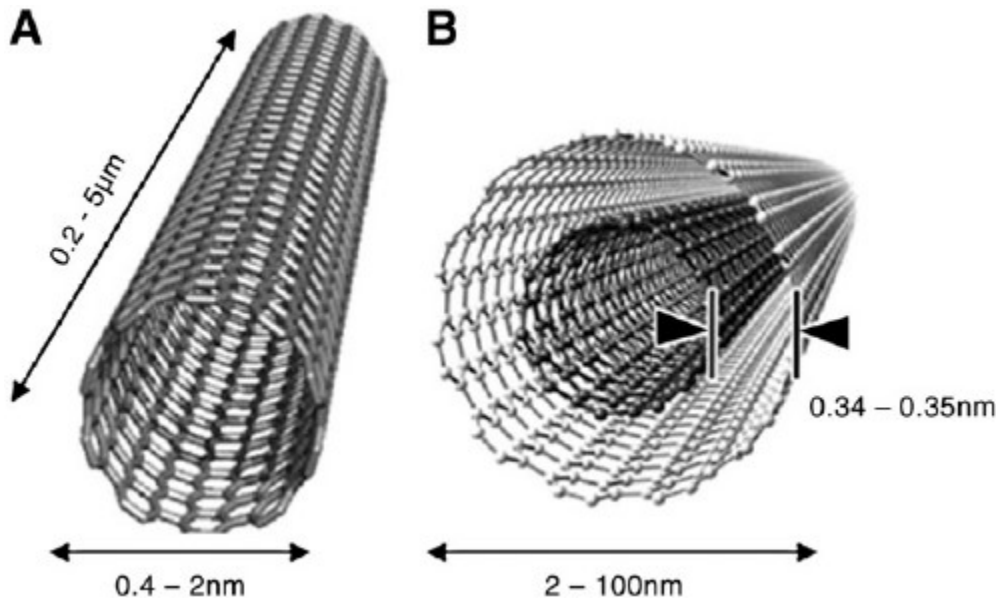

Figure 2: Types of CNTs A) SWCNT and B) MWNTs. (Figure reproduced with permission from reference 12).

Multi-walled carbon nanotubes (MWNTs)

Single-walled carbon nanotubes (SWNTs) and multi-walled carbon nanotubes (MWNTs) are main two types of carbon nanotubes (CNTs). Among these two types of CNTs, researchers showed special interest towards MWNTs. MWNTs are groups of single-walled carbon nanotube layers together. They stick together by van der Walls force. Various kinds of single-walled carbon nanotubes with different structure, shape and size can be joined together to build multi-walled carbon nanotubes (MWNTs). These single-walled carbon nanotubes (SWNTs) held together due to the pi-stacking. The single-walled carbon nanotubes (SWNTs) have distance about 0.39 nm between them, which is larger than graphene sheets distance. These layers are coupled to each other through van der Waals forces.[13] The exceptional electronic and structural properties of CNTs are importance in the field of nanomaterials-based technology and their applications. Multi-walled carbon nanotubes are mainly synthesized by chemical vapor decomposition (CVD) process. The process is inexpensive and simple. CVD method is favorable for multi-walled carbon nanotubes (MWNTs) production. Two models are used to describe multi-walled carbon nanotubes (MWNTs) structure. “Russian Doll” model and “Parchment” model. According to “parchment” model, single-walled carbon nanotubes layer is coiled around itself, like coiled paper. On the other hand, according to “Russian doll” model layers of single-walled carbon nanotubes gathered in a cylindrical structure. The distance between two single walled-carbon nanotubes in the multi-walled carbon nanotubes is about 3.4 Å.[14]

Properties of multi-walled carbon nanotubes (MWNTs)

Multi-walled carbon nanotubes (MWNTs) show exceptional mechanical and physical properties in the field of material science and nanotechnology. Multi-walled carbon nanotubes have larger length than diameter, typically 100 times larger than diameter. The quality of multi-walled carbon nanotubes (MWNTs) not only depends on diameter to length ratio, but also number of defects present in the MWNTs. The number of defects depend on the shape and entanglement of the tubes. Multi-walled carbon nanotubes (MWNTs) show excellent electronic and magnetic properties. MWNTs show increased conductivity when attached with other materials like metal oxides. Also, the sensitivity of the MWNTs can be increased during detection of analytes in electrochemical process. The sensitivity can be increased by attaching metal oxides with the MWNTs. The combined material is called composite. The outside layers of the MWNTs are conductive but the inside layers of the MWNTS are not conducting. Multi-walled carbon nanotubes (MWNTs) showed 1000 times' greater conductivity with compare to the copper. The analytes interact with the outside wall in the process of detection in sensor. Multi-walled carbon nanotubes have extraordinary structural properties. They provide strength to the composite materials. MWNTs are thermally stable up to 2800°C. Multi-walled carbon nanotubes (MWNTs) are different form of carbon, which have sp^2 hybridization. Due to the sp^3 hybridization, they show high chemical stability. Also, the stability, physical and chemical properties can be modified by functionalization of the multi-walled carbon nanotubes (MWNTs). Also, the density of multi-walled carbon nanotubes (MWNTs) can be changed by modification process. Multi-walled carbon nanotubes have also high field emission capability. Field emission is

the process to emit electrons from the surface of the material by applying voltage.[15] Therefore, they can produce high electricity from low voltage. Modified multi-walled carbon nanotubes can be used in the biosensor. Glassy carbon electrode (GCE) surface can be modified by using composite made from MWNTs. They are promising electrode materials due to the increased surface area, high chemical stability, high thermal stability and exceptional conductivity. MWNTs attached with cobalt oxide have potential application in the field of biosensors and material science.[16]

Functionalization of CNT

Pure MWNTs are not chemically active to interfere with the analytes molecules. They can be chemically active by functionalization of the surface. The functionalization process enhance sensitivity of the pure MWNTs and add some chemical properties. Pure MWNTs have no extended shape in their surface which can interact with chemical materials to combine with them. The pure MWNTs are not chemically active and need modification to make them active. But, MWNTs can be chemically active by functionalization process. Functionalization plays very important role to increase surface sensitivity of the MWNTs and functionalized MWNTs have potential application in the field of biosensor, material science and biomedicine. Functionalized MWNTs have enhanced solubility and increased dispersion properties in the solution. Also, it reduces the cytotoxicity of the pure MWNTs. The functionalized MWNTs have exceptional electrical and mechanical properties due to their high surface area and thermal stability. The functionalized MWNTs are also biocompatible. The functionalization process of MWNTs can be done using surfactants, polymers, acids, and oligonucleotides.[17] The

functionalization can be two types: covalent functionalization and non-covalent functionalization. Covalent functionalization is chemical process and non-covalent functionalization is the process to modify interfacial properties of the carbon nanotubes. Non-covalent is advantageous process than covalent process. The non-covalent process does not destroy side wall structure of the carbon nanotubes. Non-covalent functionalization was done by surfactants, polymers, aromatic compounds, etc.[18] Study shows that, functionalized MWNTs show low cytotoxicity with the attachment of surfactants than pure MWNTs. Due to the low cytotoxicity functionalized multi-walled carbon nanotubes (fMWNTs) can be used in the living cell for biological research. They have very good dispersion and low conglomeration in the cell culture with low toxicity.[19] Functionalized multi-walled carbon nanotubes also used to modify glassy carbon electrode surface to increase the sensitivity of the surface. Functionalized multi-walled carbon nanotubes have important application in the field of electrochemical sensor.

Cobalt oxide particle

Cobalt oxides have three oxidation states: cobalt (II) oxide, cobalt (III) oxide and cobalt (II, III) oxide. Cobalt oxides are transition materials. They have various electronic and magnetic properties which are important in the fields of biosensors, electronics, catalysis, solar energy etc.[20] As a transition metal oxide, they show various oxidation state with distinct chemical properties. In biosensors, they used to make composite materials incorporated with carbon nanotubes and other nanomaterials. Pure cobalt oxides show less electrochemical activity with compare to the composite materials. Cobalt (II) oxides are paramagnetic in nature. Pure cobalt oxides have less interaction

with analytes. Modification of cobalt oxide by other nanomaterials like carbon nanotubes can increase interaction with the anlaytes during electrochemical reactions. They have high density. Nanosized cobalt oxide are used to increase density in the composite materials. The increased density has also effects in the sensitivity of the composite in the electrochemical sensor. Cobalt oxides have high field emission capability. Field emission is the process to emit electron from the surface of the materials. Nanosized cobalt oxide (6-8) nm can be synthesized from the reduction cobalt (II) bis (2-ethylhexyl) sulfosuccinate. $NaBH_4$ is used as a reducing agent during reduction. Also, cobalt oxide of (8-200) nm sized can be produced using thermal decomposition process of cobalt acetate tetra hydrate. Cobalt (II) oxide can be synthesized from cobalt (II) oxide and Co particles.[21]

Composite of cobalt oxide and carbon nanotube

Composite can be prepared using cobalt (II) oxide (CoO) and carboxylic acid functionalized multi-walled carbon nanotube (COOH-MWNTs). Cobalt oxides have a lot of favorable properties to make composite. Cobalt oxides are attracting electrode materials for biosensors. They are inexpensive and naturally plentiful. As a transition metal oxide, they have excellent electronic and magnetic properties. Multi-walled carbon nanotubes also have unique electronic and structural properties, which have significant application in the field of biosensors. Cobalt oxides and multi-walled carbon nanotubes can be attached to increase sensitivity of the biosensor. Pure cobalt oxide and pure carboxylic acid functionalized multi-walled carbon nanotubes have low sensitivity. Also,

it is difficult for the pure materials to interact with the analytes molecule. Modification of carboxylic acid functionalized multi-walled carbon nanotubes (MWNTs) can increase interaction with the analyte molecules. Cobalt oxide has capability to contact with ions from bulk and surface of the materials. But due to the poor electrocatalytic activity cobalt oxide alone cannot interact with analytes effectively. But the modification process increases charge transfer capability significantly. By modification process, the composite will achieve increased surface area and conductivity towards detection of analytes. The process also increased the charge density and field emission capability. There is broad application of carbon nanotubes in the field of electrode materials and development of biosensors. The key strategy to increase the sensitivity of the functionalized multi-walled carbon nanotubes (MWNTs) by changing chemical and structural properties is surface modification. By modification, the change can be happened within van der Waals interaction, charge transfer, pi-bonding, and so on. The significant change happened in the materials due to the contribution of specific functions from each composite material. Although, pure cobalt (II) oxide (CoO) particles and pure COOH-MWNTs have poor electro-catalytic activity and sensitivity, the composite of cobalt (II) oxide (CoO) and carboxylic acid functionalized multi-walled carbon nanotubes (COOH-MWNTs) show enhance sensitivity towards the detection of dopamine.[22]

Dopamine

Dopamine (DA) is a neurotransmitter (neurotransmitters are chemical substances that carry chemical message from one nerve cell to another nerve cell in the human body) that has several important roles (motivation, habit learning, motor control, reward etc.) in the human brain. Dopamine (DA) is an important neurotransmitter in all animals, including humans. Dopamine (DA) manufactured in the kidneys and brain. In human brain dopamine manufactured in the central nervous system. Dopamine (DA) synthesized in the ventral tegmental area and released in the nucleus accumbens and the prefrontal cortex area of the central nervous system. Dopamine (DA) also found outside of the central nervous system. Outside of the central nervous system, dopamine (DA) acts as a local chemical messenger. In blood vessel, it prevents release of another neurotransmitter norepinephrine.[23] In the digestive system, it decreases insulin production. There are several neurological diseases those are related with dopamine concentration in the human brain. Unusual concentration of dopamine in human brain can cause to the reason of several severe mental disease like hyper activity disorder, Parkinson's disease, depression, schizophrenia and addiction.[24] An early detection of changes in the concentration of dopamine is important for the diagnosis and treatment of these diseases.

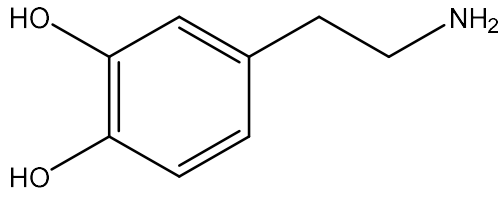

Figure 3: Dopamine (3,4-dihydroxyphenethylamine)

Detection of dopamine (DA) by CoO/MWNT composite

In the biological fluid ascorbic acid (AA) and uric acid (UA) exist with dopamine (DA). The presence of ascorbic acid and uric acid greatly interfere during the detection of dopamine. So, the detection of dopamine is very challenging with the presence of ascorbic acid (AA) and uric acid (UA).[25] There are several techniques to detect dopamine, like HPLC, UV-vis, electrochemical and fluorescence spectroscopy techniques and so on. These techniques can be used to detect dopamine in the biological fluid. But, in HPLC, GC and other spectrometry techniques, sample preparation process are very complicated, expensive and lengthy. On the other hand, electrochemical methods are cheap, fast and simple.[26] Carbon nanotubes (CNTs) and cobalt oxides are promising electrode materials in biosensor. Cobalt oxide particle incorporated with carboxylic acid functionalized multi-walled carbon nanotube (CoO/MWNTs) can be used to detect dopamine.

Analytical techniques used for the preparation of dopamine sensor

Cyclic Voltammetry (CV) is used for the detection of dopamine sensing. XPS, Raman and IR techniques are used for the characterization (CoO /COOH-MWNT) nanocomposites.

Cyclic voltammetry

Cyclic voltammetry (CV) is an analytical approach to measure current using electrochemical cell. A potentiostat is used to obtain current vs potential voltammogram. Cyclic voltammogram is found from the current, I vs potential, E curve. Current is measured with the change of potential. The change of current is happened due to the electrochemical reactions. Oxidation and reduction reaction change the current in cyclic voltammetry. Positive current of the cyclic voltammogram represents oxidation reaction and negative current of the cyclic voltammogram represent reduction reaction. There are three electrodes used in the electrochemical cell: a) reference electrode, b) working electrode and c) counter electrode. The working electrode potential is measured by using reference electrode at constant potential. **Figure 4** is showing oxidation and reduction process with the change of current. Point (a) to (d) in the cyclic voltammogram is representing reduction process and point (d) to (g) in the cyclic voltammogram is representing oxidation process. The current due to the reduction is cathodic current and the current due to the oxidation is anodic current. In the **Figure 4** i_{pc} is cathodic current and i_{pa} is anodic current. The potential E_{pc} is cathodic peak potential and the potential E_{pa} is anodic peak potential. At E_{pc}, all analytes become oxidized and at E_{pa} all analytes become reduced.

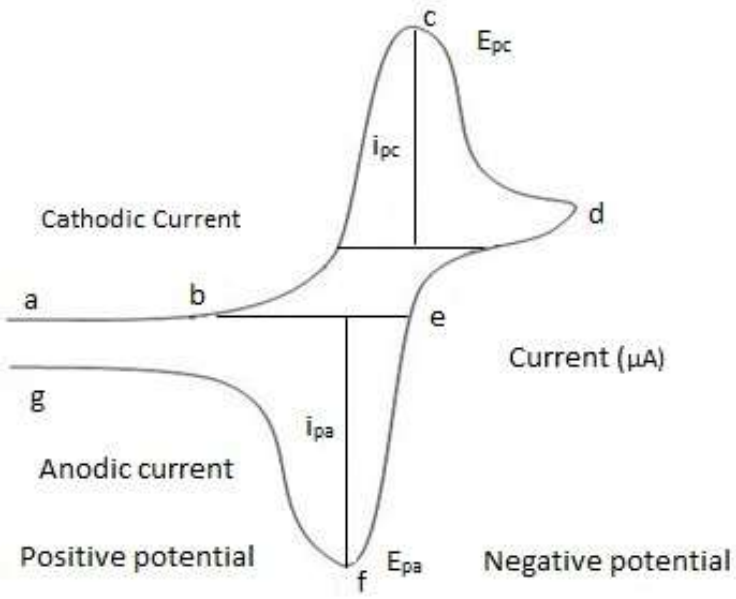

Figure 4: Typical cyclic voltammogram. Potential, V vs Reference electrode.

Figure 4 is the cyclic voltammogram with ideal duck shape. The ideal duck shape represents reversible oxidation and reduction reaction in the process. If the shape is not ideal duck shape, the redox reactions are irreversible. From peak height and peak area of the cyclic voltammogram we can measure concentration of the analytes and also represents different oxidation state of the analytes. Cyclic voltammogram is an important qualitative and quantitative analysis technique. Also, from the cyclic voltammetry we can know oxidation and reduction potential of the analytes. Cyclic voltammetry is an important identification technique. The oxidation reactions can be diffusion controlled or kinetically controlled. Using cyclic voltammetry study, we can identify the reactions either diffusion controlled or kinetically controlled.

Electrochemical mechanism of dopamine:

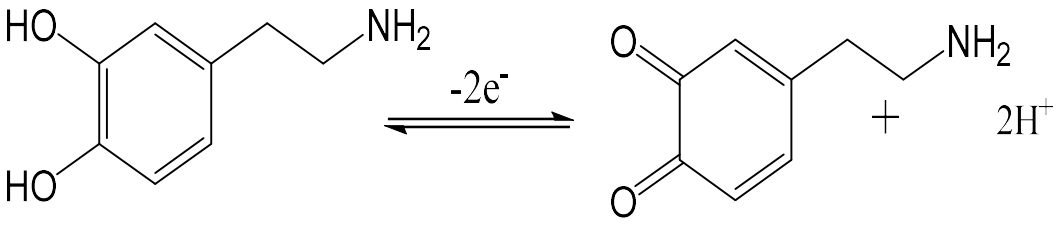

Dopamine Dopamine-o-quinone

With the increase of potential, dopamine become oxidized to dopamine-o-quinone and when potential decrease the dopamine-o-quinone become reduced to dopamine.[27]

X-ray photoelectron spectroscopy (XPS)

X-ray photoelectron spectroscopy (XPS) is a very important technique to study atomic composition and oxidation state of the elements present in the surface. In XPS analysis, an X-ray light is passed through the sample. X-ray light interacts with the surface of the materials and eject electron from the core level of elements. The energy of the ejected electrons is measured, and binding energy is calculated to determine the oxidation state of elements. The calculated binding energy is compared with the literature to identify oxidation state. Using XPS technique, it is possible to measure oxidation state of the elements, atomic composition of the sample, and empirical formula of the sample. X-ray photoelectron spectroscopy is a surface sensitive technique. The technique is mostly used to investigate surface composition. In X-ray photoelectron spectroscopy instrument, there is an electron energy analyzer. The electron energy analyzer can analyze the energy of ejected electrons. In biosensor, composite materials

used to modify the surface of the electrode. The composite surface can be characterized by X-ray photoelectron spectroscopy technique. The materials surface can be analyzed before and after modification of the materials. There is a (20-500) μm diameter beam of monochromatic K_α X-rays (Aluminum, Al) in the X-ray photoelectron spectroscopy instrument. Also, a (10-30) mm diameter beam of non-monochromatic K_α X-rays (Aluminum, Al/magnesium, Mg) can be used for the analysis. X-ray photoelectron spectroscopy can only detect the electrons, which are ejected from the surface of the sample. The ejected electrons passed through the vacuum to reach in the detector. The X-ray light interact with the sample to excitation and ejection of the electrons from the surface. Most of the traditional X-ray photoelectron spectroscopy instrument used to analysis solid sample. There are few advanced X-ray photoelectron spectroscopy instrument, which can analyze liquid and gaseous sample. X-ray photoelectron spectroscopy instrument can make cool/ hot the sample before and during analysis.[28, 29]

Infrared spectroscopy

Infrared spectroscopy (IR) is a characterization technique that use infrared light to analysis sample. In infrared spectroscopy, infrared ray interacts with the sample during analysis. It is also called vibrational spectroscopy technique. IR spectroscopy is an important technique to identify functional groups present in the sample. IR spectroscopy can be used for solid, liquid and gaseous samples. A spectrophotometer is used to produce infrared ray in the infrared spectroscopy. Fourier transform infrared spectrophotometer (FTIR) is the popular instrument used in the infrared spectroscopy.

There are three regions in infrared spectrum region: near IR, mid IR and far IR. These regions are corresponding to the visible light region. Also, these three regions have different electromagnetic properties. Infrared light is passed through the sample to analysis sample. When the frequency of the infrared light matched with the vibrational frequency of the bonds present in sample, sample absorbed infrared light. The energy of the absorbed infrared energy is measured using a monochromator to get the spectrum. Also, a band of wavelength region can be measured using Fourier transform infrared spectroscopy (FTIR). Infrared analysis is used to study covalent bonds in the chemical structures. Attenuated total reflectance infrared spectroscopy (ATR-IR) is used to analysis solid sample. There are two regions in infrared spectroscopy: functional groups region and fingerprint region. Maximum information is found from the infrared spectrum at functional groups region. Fingerprint region is complicated to interpret, and fingerprint region is identical for every functional groups. Polar covalent bonds are mainly infrared active, and they represent the functional groups in organic molecule. [30, 31]

Raman spectroscopy

Raman spectroscopy is also a characterization technique by Raman scattering/inelastic scattering. Raman spectroscopy also a vibrational spectroscopy technique. Raman spectroscopy is important to study low-frequency modes of the matter. Rotational and vibrational frequency can be studied by using Raman spectroscopy technique.[31] A beam of light passed through the sample during analysis using a monochromator in Raman spectroscopy. The light can be near IR, near UV or visible light. A laser is used as monochromator light source. Raman spectroscopy is used to

acquire structural information to understand molecule. It also provides fingerprint information which are identical for every molecules. In Raman spectroscopy, light interacts with the matter to make Raman shift of photons. The Raman shift provides information about vibrational frequency. Raman spectroscopy is a similar type of vibrational spectroscopic technique like infrared spectroscopy. During Raman analysis, a beam of laser light is passed through the sample and sample molecule interact with the laser light. A monochromator is used to produce laser beam. Lights, after interaction with the sample filtered and pass through the detector. By Raman spectroscopy, solid sample can be characterized. In biosensor, Raman spectroscopy is used to characterized composite materials. Composite materials are used to modify the electrode surface to increase sensitivity of the biosensors. Materials characteristic can be studied using D-to-G band ratio found from the Raman spectra. Disordered sp^3 hybridized carbon or ordered sp^2 hybridized carbon amount can be found from D-to-G band ratio. Also, electroactive surface area is related with the D-to-G band ratio.[32]

Transmission electron microscopy (TEM)

Transmission electron microscopy (TEM) is an optical characterization technique in which a beam of electrons is passed through the specimen to get image of the specimen in micro to atomic level. German physicist Ernst Ruska was awarded Novel Prize for the development of TEM in 1986. The TEM grids are used to hold the specimen during analyses. The specimen should be less than 100 nm thickness or a suspension on the grid to get good TEM images. An image is formed due to the interaction of electrons with the specimen. Imaging device such as fluorescent screen, layer of photographic film, charge-

coupled-device are used to focus and magnified images. Transmission electron microscopy can create thousand times smaller image than the real image. It makes scientists enable to study sample even at an atomic level. It needs very low pressure about 10^{-4} to 10^{-7} Pa to perform operation. An electron gun is used to produce electron beams and electron lens are used to focus and magnify images. Transmission electron microscopy is capable to take image at very high resolution compare to the other light microscopes. Transmission electron microscopy is a very important technique in material science, biological science, nanotechnology, semiconductor and cancer research. We used transmission electron microscopy in this thesis to study morphology of the materials and measure the average particle size.[33]

Research objective

An early detection of changes in the dopamine concentration is important for identification of neurological diseases and their treatments. *In situ* and real-time quantification of neurotransmitters by a neuronal-solid-state device would revolutionize research in neurological diseases and their treatments. In this work, a novel electrochemical dopamine sensor based on COOH-functionalized multi-walled carbon nanotubes (COOH-MWNTs) incorporated with Cobalt oxide nanoparticles will be prepared and the electrocatalytic behavior of the sensor will be investigated using cyclic voltammetry technique. Characterization of CoO/COOH-MWCNTs nanocomposite will be done using XPS, IR, and Raman spectroscopy techniques. The extraordinary structural, mechanical, and electrochemical properties of carbon nanotubes coupled with several desirable properties of cobalt oxide (CoO) nanoparticles having a high

conductivity, wide band gap, high exciton binding energy, and fast electron transfer characteristics render the CoO/COOH-MWCNTs composites highly promising materials for electrochemical sensor applications. The CoO/COOH-MWCNTs nanocomposite showed excellent electrocatalytic activity, rapid response time and good sensitivity toward the detection of dopamine.

CHAPTER II

EXPERIMENTAL

In this research, an electrochemical sensor was developed to detect dopamine. First, a cobalt oxide attached with carboxylic acid functionalized multi-walled carbon nanotube (CoO/COOH-MWNT) composite was prepared by combining COOH-MWNTs and cobalt oxide (CoO) particles. Cobalt oxide particles and COOH-MWNTs were combined by sonication process in absolute anhydrous ethyl alcohol (AAEA) to make a colloidal suspension of CoO/COOH-MWNT composite. Cobalt oxide powder and functionalized multi-walled carbon nanotubes (COOH-MWNT) were mixed in 1:1 ratio. Then, the CoO/COOH-MWNT composite was used to increase the sensitivity of the mirror like electrode surface. Different electrochemical studies of dopamine by using CoO/COOH-MWNT/GCE electrochemical sensor were done to observe the sensitivity of the developed sensor. Studies were done changing different parameters like concentration of the dopamine solutions, pH of the dopamine solutions, sonication time of the combining cobalt oxide and functionalized multi-walled carbon nanotubes (COOH-MWNT). Finally, different elemental and optical analyses were done to characterize the sensor. X-ray photoelectron spectroscopy (XPS) analysis was done for elemental analyses. Optical characterization of the CoO/COOH-MWNT/GCE electrochemical sensor was done by ATR-IR, Raman spectroscopy and TEM analyses. **Scheme-1** shows a flow chart to briefly describe the research methodology applied in this thesis to develop the electrochemical dopamine sensor.

Scheme 1: Flow chart of research process for the development of dopamine sensor.

Different instruments used for analysis

Instruments used in this research for different analysis purpose:

a. Digital analytical balance (Mettler AE-163, New Jersey, USA)

b. Ultrasonic Cleaner (Sharpertek Stamina XPTM, WI, USA)

c. Water de-ionizer (ELGA, High Wycombe, UK)

d. pH meter (Thermo electron corporation, Orion 230 A+, MA, USA)

e. Oven (Thelco Laboratory, CA, USA)

f. Magnetic Stirrer (Fisher Scientific, MA, USA)

g. WaveNano USB Potentionstat (Pine instrumentation, Raleigh, NC, USA)

h. Attenuated total reflection spectroscopy (Varian-7000 FTIR, MA, USA)

i. Raman spectroscopy (Enwave Optronics, Inc., Model-uSense-I-785, Irvine, CA, USA)

j. X-ray photoelectron spectroscopy, XPS (Perkin Elmer PHI 560, MA, USA)

k. Transmission electron microscopy, TEM (Hitachi H-7650, Krefeld, Germany)

Chemicals and materials

Different chemicals and materials were used during experiments:

a. COOH-MCWNTs (Nano Lab, Inc., Walton, MA, USA)
b. Cobalt oxide (Nanostructured and Amorphous Materials (99% purity), Los Alamos, New Mexico, USA)
c. Dopamine (Sigma-Aldrich, St. Louis, MO, USA)
d. Glucose (Sigma-Aldrich, St. Louis, MO, USA)
e. L–Ascorbic Acid (Sigma-Aldrich, St. Louis, MO, USA)
f. 4–Acetamidophenol (Sigma-Aldrich, St. Louis, MO, USA)
g. Folic Acid (Sigma-Aldrich, St. Louis, MO, USA)
h. Nafion (Ion Power, Inc, New Castle, Delaware, USA)
i. Sodium Chloride (Fisher Scientific, Pittsburgh, USA)
j. Hydrochloric Acid (Fisher Scientific, Pittsburgh, USA)
k. Absolute anhydrous ethyl alcohol (AAEA) \(Pharmco-AAPER, Brookfield, CT)
l. Micropolish^{TM} Alumina, 0.05 μM (Lake Bluff, IL,USA)
m. Micropolish^{TM} Alumina, 1.00 μM (Lake Bluff, IL,USA)
n. Phosphate Buffer Solution (PBS), pH 7.00 (Sigma-Aldrich, St. Louis, MO, USA)
o. Buffer Solution, pH 4.66 (EMD Millipore Corporation, Billerica, MA, USA)

CoO/COOH-MWNT composite preparation

First, functionalized multi-walled carbon nanotubes (COOH-MWNT) (2 mg) and cobalt oxide (2 mg) were taken to make 1:1 mixture. The mixture is then sonicated in 1 mL of AAEA to get the colloidal solution. The resulting solution is the CoO/COOH-MWNT composite which was used to change the GCE surface. Only, COOH-MWNT remained uniformly dispersed in AAEA solution after the sonication. But, CoO/COOH-MWNT composite have precipitation within 5 min. due to the sonication. The COOH-MWNTs showed enhanced density due to attachment of the CoO to the COOH-MWNTs. The electrocatalytic oxidation and reduction of dopamine studied at 15 min. to 60 min. sonication times with cyclic voltammetry. The CoO/MWNTs composite showed highest sensitivity at the 30 min. sonication time with compare to the 15, 45 and 60 min. sonication time. Also, the electrocatalytic oxidation and reduction of dopamine was studied for different concentrations of dopamine solutions at different pH values.

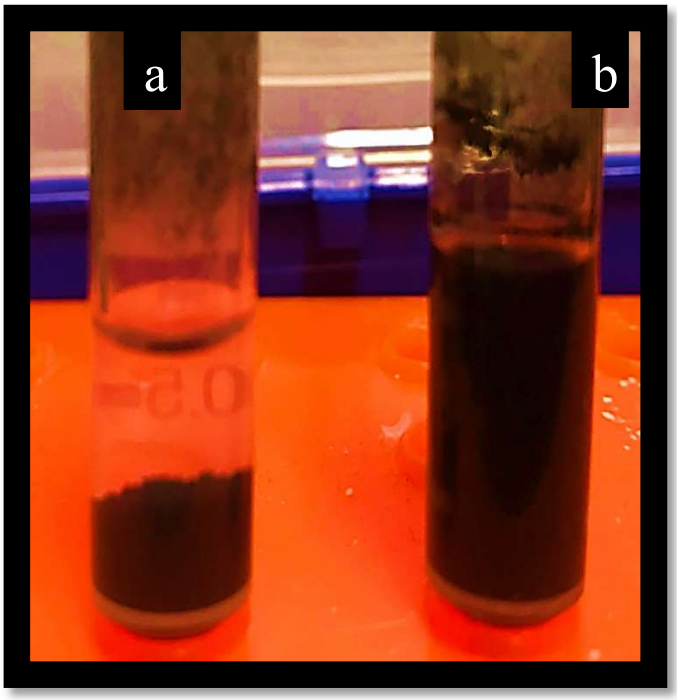

Figure 5: Sedimentation of materials after sonication

a) CoO/COOH-MWNT composite sedimentation, b) pure CoO has no sedimentation.

Attaching CoO/COOH-MWNT composite with glassy carbon electrode for electrochemical sensing

The CoO/COOH-MWNT suspension attached above the GCE surface using the process reported in Wayu *et al*.[34] A drop casting method was used to modify the GCE

surface using CoO/COOH-MWNT composite suspension. First, the glassy carbon electrode (GCE) surface was polished using 1.0 μm and 0.05 μm diameter alumina slurries for about 10 minutes each time to get the mirror like electrode surface. Then, GCE surface was washed using ultrapure deionized water and the surface was cleaned by 5 min. of sonication. Also, the electrode surface was sonicated using concentrated nitric acid: deionized water 1:1 for 5 min. to activate the surface. The GCE surface was then dried using Kim-wipes at room temperature. After that, the vial of CoO/COOH-MWNT composites suspension was shaken few minutes to get uniform suspension of CoO/COOH-MWNT composites. Then a 10-μL aliquot of suspension was applied to the electrode. The measured amount of CoO/COOH-MWNT composite suspension then dropped onto the previously polished mirror like electrode surface. The electrode was then dried in oven for 10 minutes at 80ºC so that the CoO/COOH-MWNT composite was coated on the electrode surface. The mirror like electrode surface became black after the treatment. Another 10-μL aliquot of the Nafion (2% wt) in AAEA solution was measured using micropipette. The measured solution was dropped on to the previously prepared black electrode surface. The Nafion (2% wt) in ethyl alcohol was used to bind the electrode surface with CoO/COOH-MWNT composites suspension. The above modified electrode was then dried in oven at 80ºC for another 10 minutes. Finally, the Nafion/CoO/COOH-MWNT/GCE electrochemical sensor was made to detect dopamine.

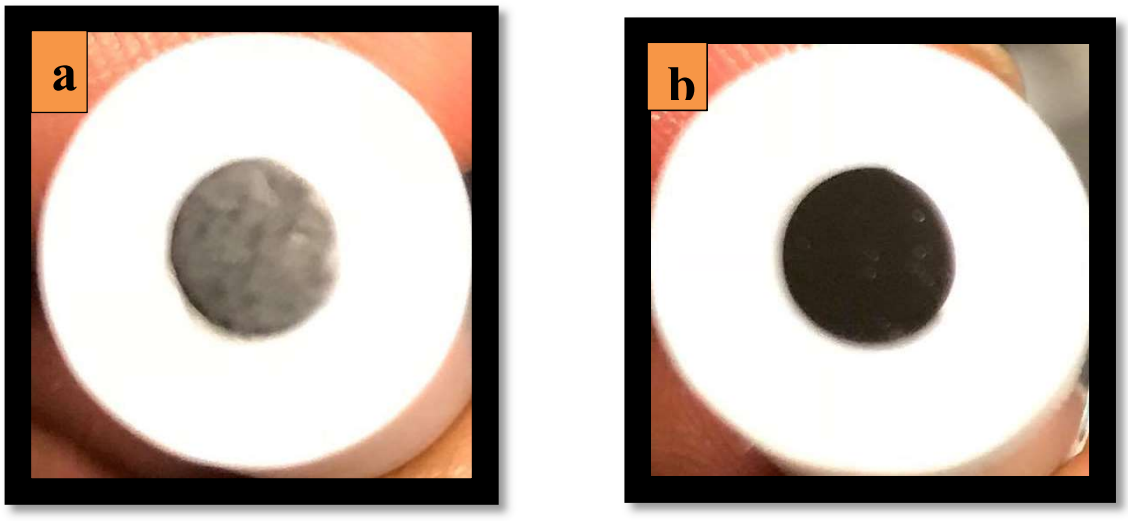

Figure 6: Glassy carbon electrode (GCE) surface

a) Before attaching composite (mirror like surface), and b) after attaching Composite.

Electrochemical study of dopamine using CoO/COOH-MWNT/GCE sensor

Electrochemical study of dopamine using CoO/COOH-MWNT/GCE sensor was performed using cyclic voltammetry (CV). The cyclic voltammetry experiment was done inside a custom-built Faraday cage. An inert atmosphere of N_2 gas at room temperature 22 ± 1 °C was maintained for the electrochemical cell. The range for potentials was set at -0.10 to +0.10 V and scanning was performed at 50 mV/s rate during CV experiments. Wave Nano potentiostat and Aftermath (Version 1.4.7881) electrochemical software (Pine Instruments, Raleigh, NC, USA) were used during CV experiments. Cyclic voltammetry experiments were carried out using an electrochemical cell which consists of three electrodes. The three electrodes included a reference electrode (Ag/AgCl (3.5 M KCl)), a Pt wire counter electrode and the previously prepared CoO/COOH-MWNT/GCE. CV experiments were done at specific peak potential for dopamine. Two different buffer solutions were used during CV experiments. PBS of pH 7.0 (Sigma-Aldrich, St. Louis, MO, USA) and buffer solution of pH 4.66 (EMD Millipore Corporation, Billerica, MA, USA) were used during all electrochemical measurements of dopamine. Ultra-pure deionized water was used to prepare all solutions. All chemicals used were of reagent grade. Dopamine, ascorbic acid, and uric acid were bought from Sigma Aldrich (St. Louis, MO, USA).

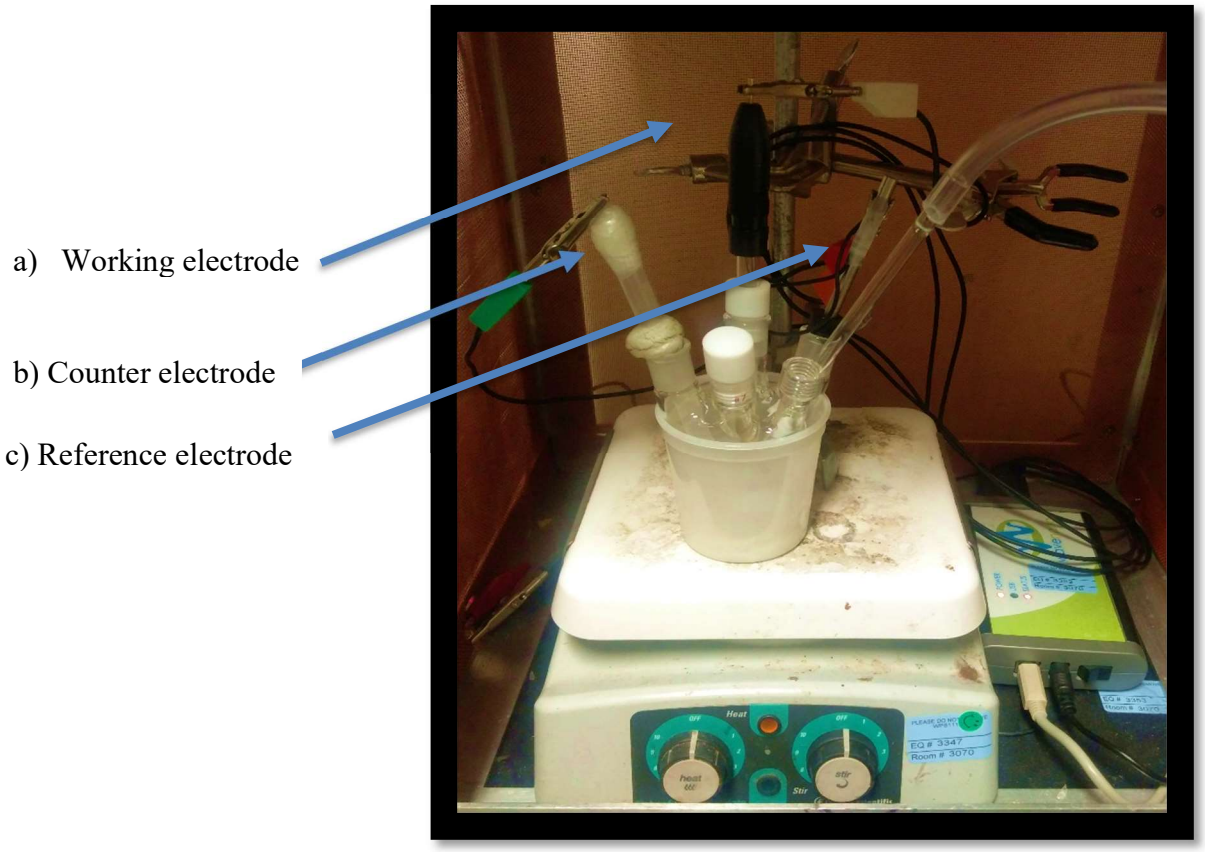

Figure 7: Electrochemical cell used during cyclic voltammetry experiments. a) Working electrode, CoO/COOH-MWNT/GCE, b) Counter electrode, a Pt wire, c) Reference electrode, Ag/AgCl (3.5 M KCl).

X-ray photoelectron spectroscopy (XPS) analysis of CoO/COOH-MWNT solid composite

The elemental analyses of CoO/COOH-MWNT solid composite was performed by X-ray photoelectron spectroscopy (XPS). First, a fine powder of CoO/COOH-MWNT solid composite was prepared by crushing and grinding. Then the uniformly crushed powder was fixed on the XPS sample holder using scotch tape (Scotch 3M). The sample holder was then outgassed in a turbo-pumped antechamber before experiments. Up to 7.0 x 10^{-9} Torr pressure of the system was maintained during experiments. XPS experiments of the CoO/COOH-MWNT composite was done using a Perkin-Elmer ESCA PHI 560 instrument. Mg Kα anode was used to generate non-monochromatic X-rays during experiments. The photon energy of the Mg Kα anode was 1253.6 eV. The PHI 25-270AR analyzer inside the instrument was operated at 250 W and 15 kV during experiment. CasaXPS software, version 2.2.107 (Devon; United Kingdom) was used to study XPS spectra of the CoO/COOH-MWNT composite. Touggard and Shirley background subtractions were used for C 1s, O 1s, and Co 2p orbitals spectra. Also, Touggard and Shirley background subtractions were used for (30 to 70) % Gaussian-Lorentzian lines. C 1s orbital has binding energy (BE) at 284.4 eV. The presence of graphene sheets in the CoO/COOH-MWNT composite confirmed from the binding energy (BE) of the C 1s orbital.

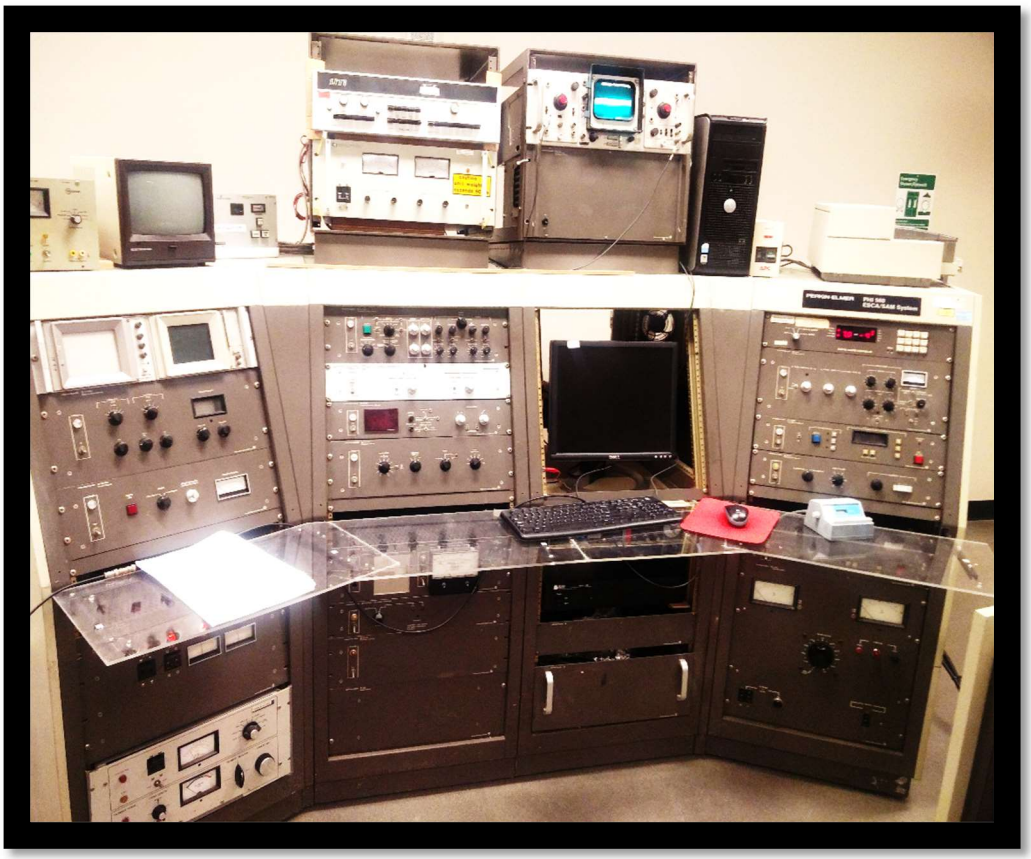

Figure 8: X-ray photoelectron spectroscopy (XPS) instrument in Dr. Chusuei's lab.

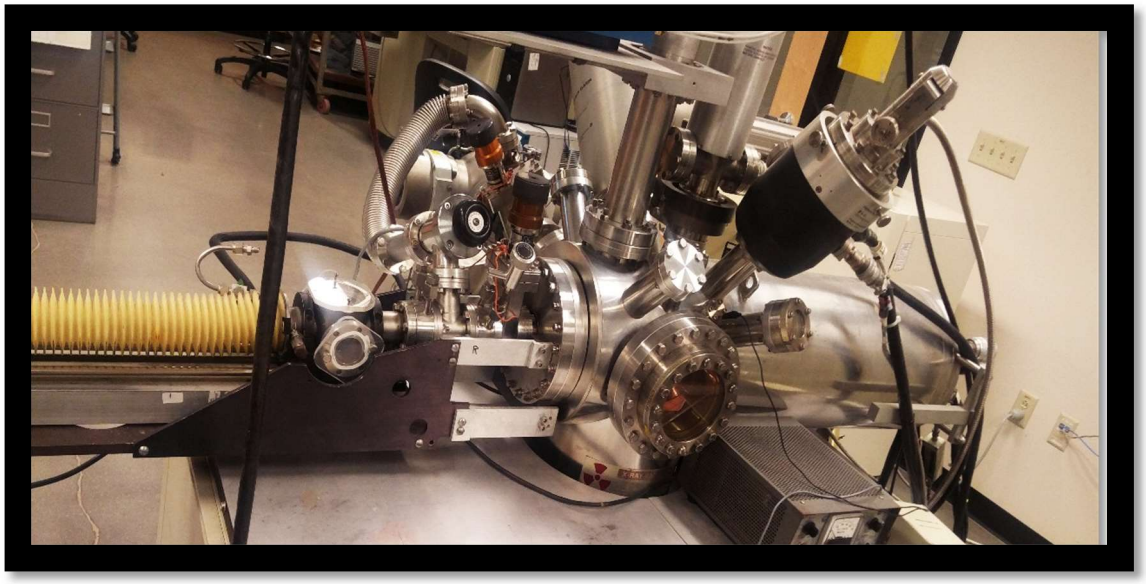

Figure 9: XPS Chamber.

Characterization of the CoO/COOH-MWNT composite

Also, The CoO/COOH-MWNT composite was characterized using TEM, ATR-IR and Raman spectroscopy. The transmission electron microscopy (TEM) technique was used to obtain CoO particle size distribution on multi-walled carbon nanotubes (COOH-MWNT) at CoO/COOH-MWNT composites. The TEM analyses of the CoO/COOH-MWNT composites were carried out using a Hitachi H-7650 TEM instrument. First, CoO/COOH-MWNT composite samples was prepared at different sonication times. Functionalized multi-walled carbon nanotubes (COOH-MWNT) (2 mg) and cobalt oxide (2 mg) were taken in 1:1 ratio and sonicated in absolute anhydrous ethyl alcohol (AAEA) to make a colloidal suspension. Drops of the prepared colloidal suspension of CoO/COOH-MWNT composite was casted on 200 mesh TEM grids (SPI supplies, West Chester, PA, USA). The grids are made of copper and carbon-coated. The CoO/COOH-MWNT composite containing TEM grids was then air dried. A lamp can be used to support the drying. The TEM grids was put in the TEM sample holder and passed through the vacuum system inside TEM chamber. A beam of electrons passed through the CoO/COOH-MWNT composite containing grid to get the images. ImageJ software (version 1.47) was used to analyze TEM images of CoO/COOH-MWNT composite samples obtained at different sonication times. The images were calibrated in Image J software at nanometer scale before measuring diameters of particles. Average diameter of CoO particles was measured 78 to 131 nm. The CoO particles was purchased from nanostructured and Amorphous Materials (99% purity), Los Alamos, New Mexico, USA.

Figure 10: Transmission electron microscopy, Hitachi H-7650 in Dr. Miller's lab.

ATR-IR experiments were done using Varian 700 FTIR instrument. Varian Resolution Pro software version 5.0. used to obtain the IR spectra. First, CoO/COOH-MWNT composite suspension was prepared at a 30 min. sonication time. The samples was prepared in AAEA taking COOH-MWNTs (2 mg) and cobalt oxide (2 mg) in 1:1 ratio. Mercury cadmium telluride (MCT) detector was used during experiment. Liquid N_2 use to cool the detector to improve the signal-to-noise ratio of the FTIR signal. Sample was placed on ATR crystal during analysis. Absolute anhydrous ethyl alcohol (AAEA)

was used as background. Finally, IR data were recorded for CoO/COOH-MWNT composite suspension obtained after 30 min. sonication period.

Raman Spectroscopy experiments were performed using Raman spectrometer (Enwave Optronics, Inc.) with laser excitation at 785 nm. A solid CoO/COOH-MWNT composite sample was prepared for Raman analyses. The solid composite samples were placed in the sample stage. The maximum power of laser source is 500 mW. Laser beam produced from source was collimated onto the solid CoO/COOH-MWNT composite sample to obtain Raman spectra. A highly sensitive CCD detector is used in the instrument. The laser light interacts with molecular vibration of the composite samples to produce Raman spectra. Data was recorded for solid CoO/COOH-MWNT composite sample at different sonication times.

CHAPTER III

RESULTS AND DISCUSSION

Elemental analyses of the CoO/COOH-MWNT composite was studied by XPS. Characterization of the CoO/COOH-MWNT composite was done by Raman spectroscopy, TEM and ATR-IR. Average CoO particles size were measured by TEM analyses. The electrocatalytic behavior of the CoO/COOH-MWNT sensor towards dopamine (DA) was carried out using cyclic voltammetry.

Attachment of CoO particles with COOH-MWNT

In **Figure 11,** there is two spectra from infrared analysis. (A) CoO/COOH-MWNT composite at 30 min. sonication and (B) pure functionalized carbon nanotubes (COOH-MWNTs) without attaching CoO particles. Pure functionalized multi-walled carbon nanotube's (COOH-MWNT) ATR-IR spectrum (Bottom-most panel of the **Figure 11**) was taken from Mulugeta's thesis and compared with CoO/COOH-MWNT composites spectrum. Pure functionalized multiwalled carbon nanotubes (COOH-MWNT) shows two peaks at 1641 cm^{-1} and 1691 cm^{-1}. The peak at 1641 cm^{-1} belongs to the C=C stretching vibration of the COOH-MWNT graphene sheet and the peak at 1691 cm^{-1} belongs to the vibration of COOH group (C=O stretching). The combination of CoO particles with COOH-MWNT does not show any peaks (Top-most panel of the **Figure-11**). The absence of the two important peaks[35] indicates that the COOH functional group of COOH-MWNT take part in the attachment of the CoO particles. Also, modified CoO/COOH-MWNT/GCE electrochemical sensor showed greater sensitivity toward the

detection of dopamine with compare to the COOH-MWNT/GCE electrode during cyclic voltammetry experiments.

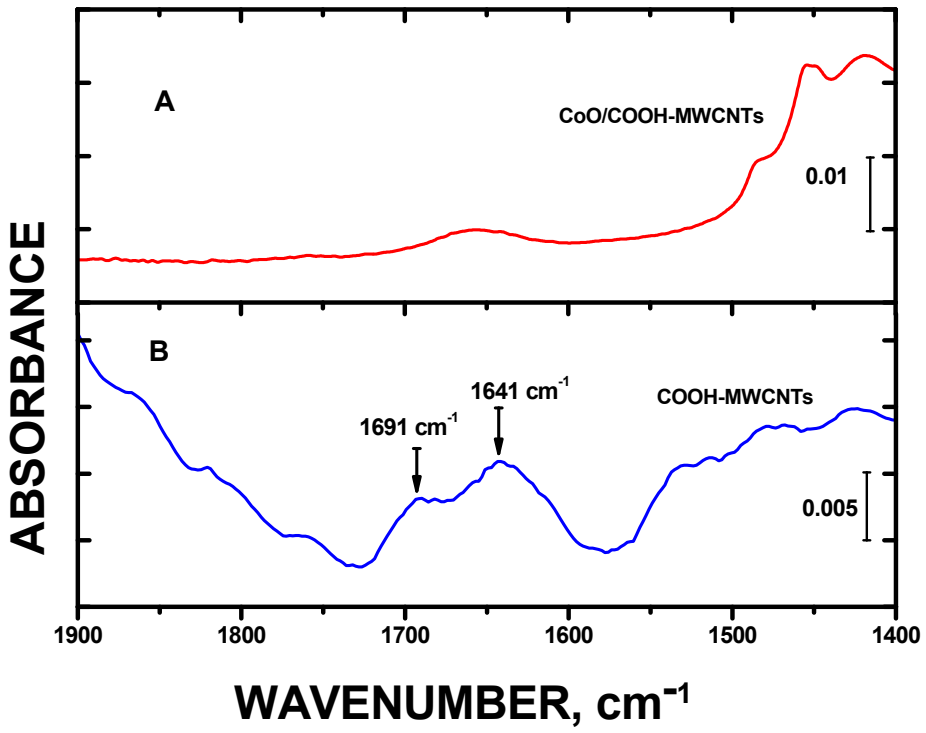

Figure 11: ATR-IR spectra of (A) CoO/COOH-MWNT composite, and (B) pure COOH-MWNT.

Raman spectroscopy analysis of CoO/COOH-MWNT composite

Figure 12 shows Raman spectra at different sonication time. The D-to-G integrated peaks in Raman spectra are used to study the degree of disordered sp^3-hybridized carbon in the MWNT. The D band and G band peaks are at 1325 cm^{-1} and 1625 cm^{-1}. The D bands at 1325 cm^{-1} is related to disordered sp^3-hybridized carbon and the G bands at 1625 cm^{-1} is related to ordered sp^2-hybridized carbon. The relative area ratio of D-to-G bands is related to the degree of disordered sp^3-hybridized carbon in MWNT. The D-to-G bands ratio is at a maximum at 30 min. of sonication. It means there is higher amount of disordered sp^3-hybridized carbon in MWNT at 30 min. of sonication.

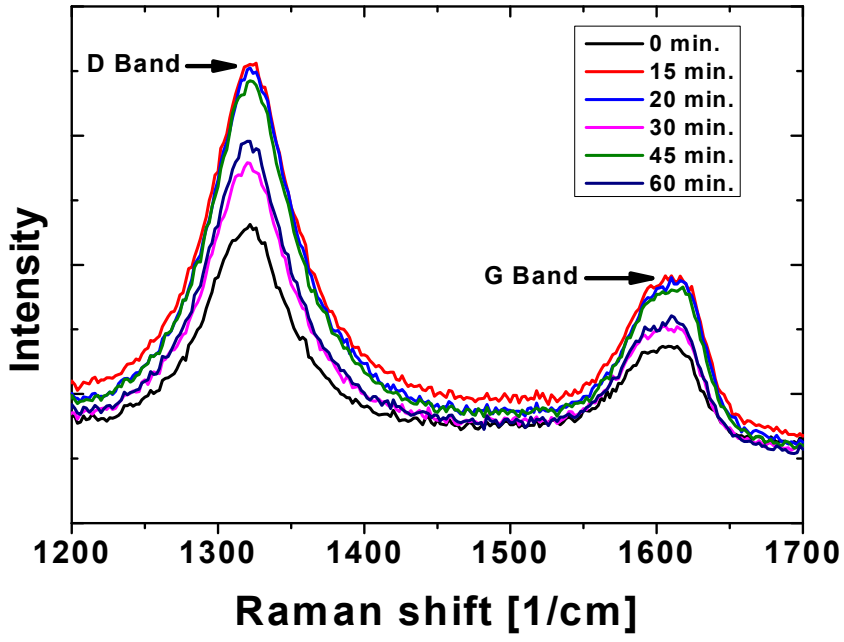

Figure 12: Raman spectra of CoO/COOH-MWNT at 0 min. to 60 min. sonication.

From **Table 1,** the disordered sp^3-hybridized carbon raised up to 30 min. sonication time, then decreased after that point. That means maximum number of disordered sp^3-hybridized graphene sheet presents at 30 min. sonication that exposed from the surface of MCNT. Cyclic voltammetry experiments also show that the 30 min. sonicated composite has the best electrochemical response. Therefore, there is an observed direct relationship between disordered sp^3-hybridized carbon and the sensitivity of CoO/COOH-MWNT composite.

Table 1: The D-to-G band ratio at various sonication.

Sonication time (min.)	D band	G band	D-to-G ratio
0	**10930**	**5571**	**1.96**
15	**17670**	**6831**	**2.58**
20	**18040**	**7258**	**2.49**
30	**13760**	**5320**	**2.59**
45	**17370**	**6923**	**2.51**
60	**14290**	**5571**	**2.57**

Figure 13 shows the plot of D/G peak integrated area ratio vs sonication time. The D-to-G peak integrated area ratio found for 30 min. of sonication is 2.59 which is the maximum as compared to other D-to-G peak ratios.

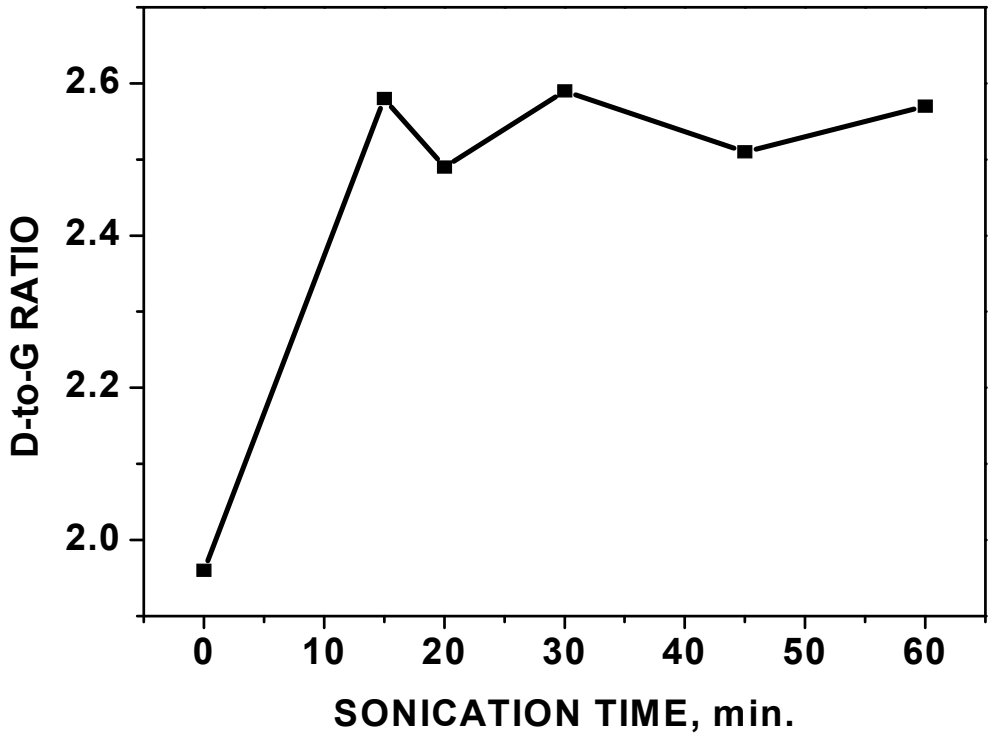

Figure 13: Plot of D-to-G peak integrated area ratio vs sonication time.

Elemental analysis of CoO/MWNT composite

XPS is an elemental characterization technique used to characterize the top-most surface elements in the materials. XPS technique is used in this thesis to study surface layers (50-100Å) of the CoO/COOH-MWNT composite. Cobalt, oxygen, and carbon from CoO/COOH-MWNT composite was identified by comparing their characteristic

peaks with the standard binding energy values. First, CoO/COOH-MWNT composites was scanned to get the survey spectrum at 0−1000 eV range. The survey study confirmed the presence of cobalt, oxygen, and carbon in the CoO/COOH-MWNT composite. Finally, narrow scans were performed at high resolution to get the individual spectrum of Co 2p, C 1s, and O 1s orbitals. The XPS study also showed the atomic percentage at top most surface of the CoO/COOH-MWNT composite. 97.03% C 1s, 2.83% O 1s and 0.14% Co 2p was found from XPS analysis.

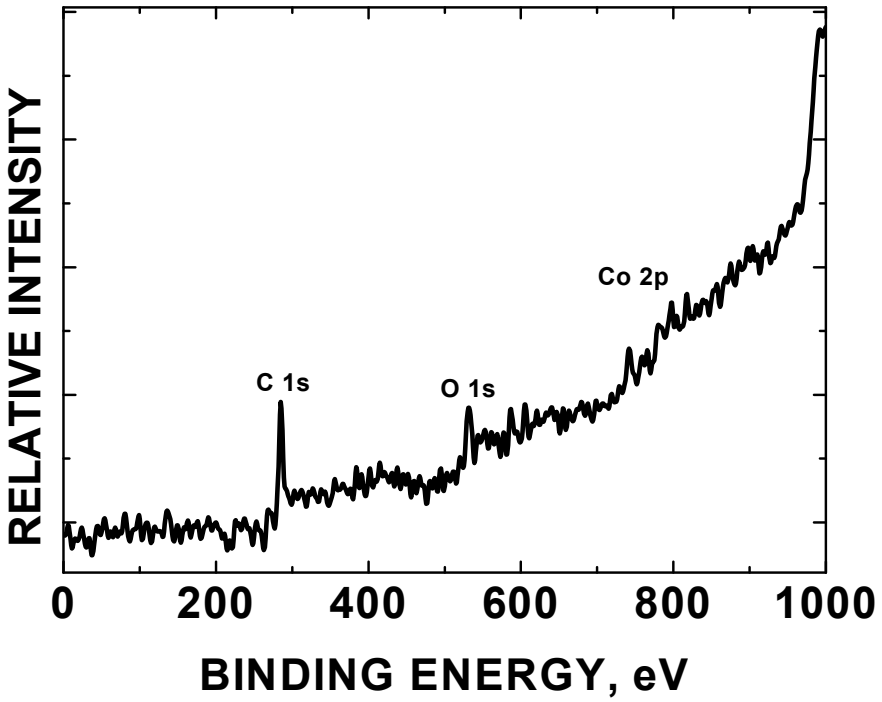

Figure 14: Survey scan of the CoO/COOH-MWNT.

Figure 14 is showing the survey scan of the CoO/COOH-MWNT composite. Co 2p, C 1s, and O 1s were identified from the survey scans.

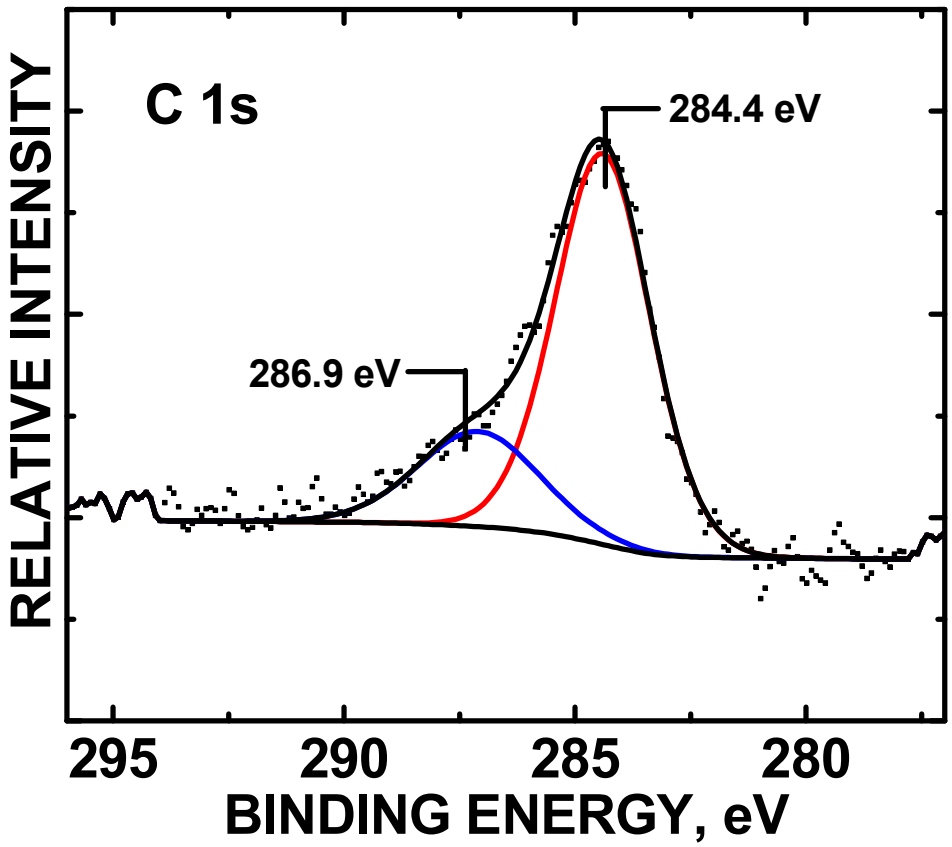

Figure 15: C 1s orbital spectrum of the CoO/COOH-MWNT from XPS analysis.

Figure 15 shows the C 1s orbital spectrum from the CoO/COOH-MWNT. The spectrum is showing two major peaks at 284.4 eV (2.5) and 286.9 eV (4.2) position. The major peak shows at 284.4 eV binding energy indicates the presence of sp^2 C-C/or C-H

orbital (graphene) in the COOH-MWCNTs.[36] The peak at 286.9 eV (4.2) position corresponds to the carbon atoms of C-O (COOH group) of COOH-MWNT.[37]

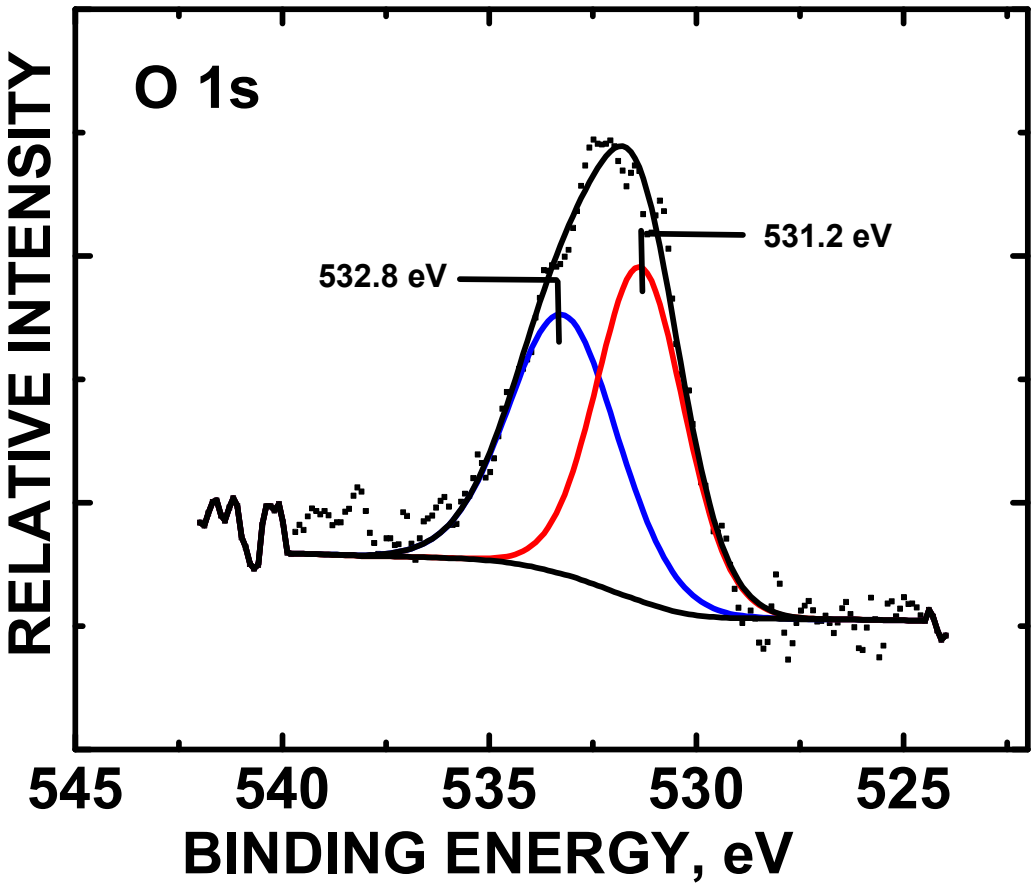

Figure 16: O 1s orbital spectrum of the CoO/COOH-MWNT from XPS analysis.

Figure 16 shows O 1s orbital spectrum of the CoO/COOH-MWNT. The spectrum shows two peaks at around 531.2 eV (2.3) and 532.8 eV (3.5) position are due to the single and double bond oxygen.[38] The peak at 531.2 (2.3) position due to the keto group

present in the composite[39] and the peak at 532.8 (3.5) eV indicates the presence of hydroxyl oxygen[40] in the composite.

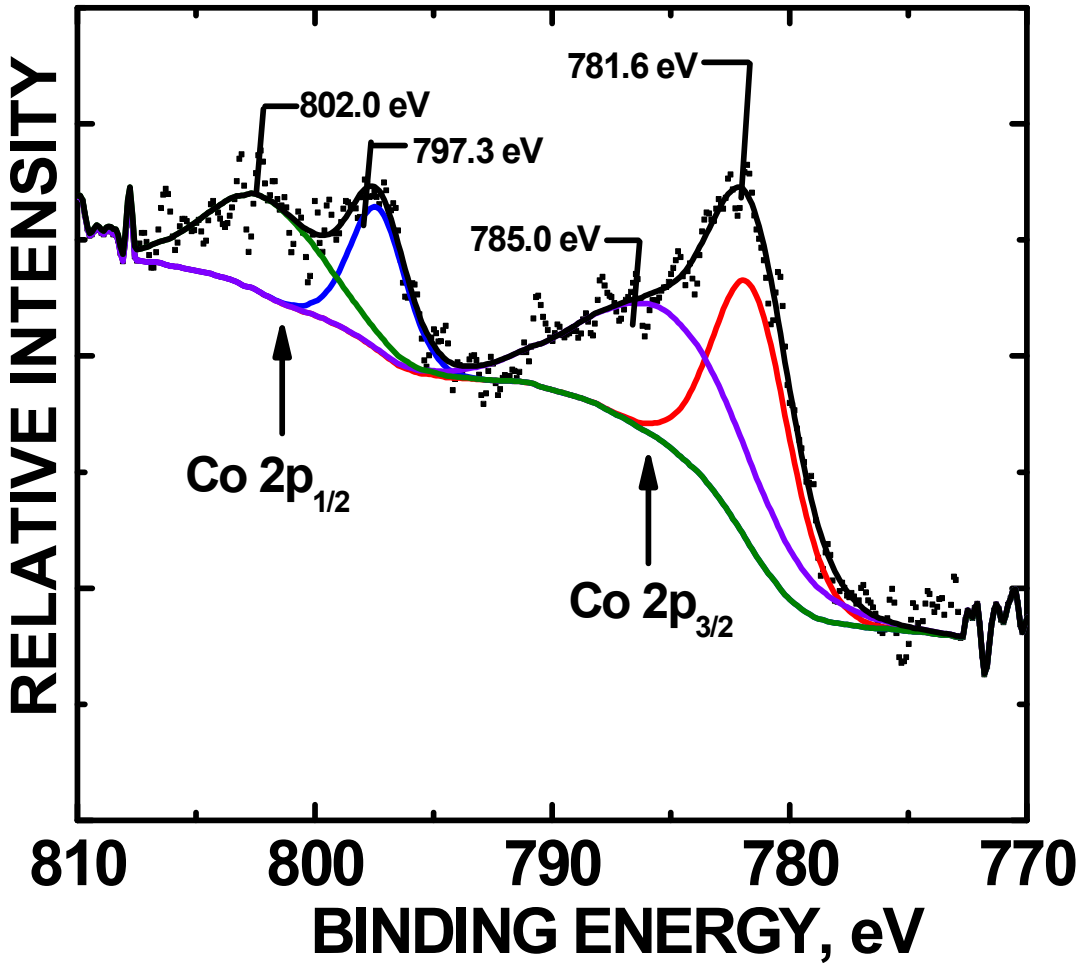

Figure 17: Co 2p orbital spectrum of the CoO/COOH-MWNT from XPS analysis.

Figure 17 shows Co 2p XPS spectum of the CoO/COOH-MWNT. The figure also shows spin orbital splitting of Co 2p orbital. Split Co $2p_{1/2}$ and Co $2p_{3/2}$ peaks has

also shake-up structure at high energy, which indicate that Co^{2+} has paramagnetic nature[41]. Co $2p_{1/2}$ has two peaks at 802.4 eV and 797.7 eV and Co $2p_{3/2}$ shows two peaks at 786.4 eV and 781.8 eV. The BE of Co $2p_{1/2}$ and Co $2p_{3/2}$ are 797.7 and 781.8 eV respectively. The spin orbit coupling ΔE (Co $2p_{1/2}$ - Co $2p_{3/2}$) is 797.7-781.8 = 15.9 eV, which is the characteristic of CoO.[42, 43, 44]

Table 2: XPS data for the CoO/COOH-MWNT composite.

Element	Fitted area	No. of scans	Normalized area	Atomic %	Peak position and fwhm
C 1s	3406.6	318	52.3	97.03	284.4 eV (2.5), 286.9 eV (4.2)
O 1s	1456.3	1516	1.5	2.83	532.83 eV (3.5), 531.2 eV (2.3)
Co 2p	1435.5	4133	0.08	0.14	781.6 (3.8), 797.3 (2.8), 785.0 (8.4), 802.0 (5.9)

Transmission electron microscopy (TEM)

We found best current response for 30 min. sonication time during CV experiment as compared to 15, 20, 45 and 60 min. sonication times. To investigate the morphology of the composites at different sonication time we acquired TEM images of CoO/MWNT composites. **Figure 18, 20, 22, 24, 26, 28** show TEM images and size distribution histograms of CoO/COOH-MWNT at 0 (without sonication), 15, 20, 30, 45 and 60 min. sonication times. Sonication experiments were carried out in absolute anhydrous ethyl alcohol.

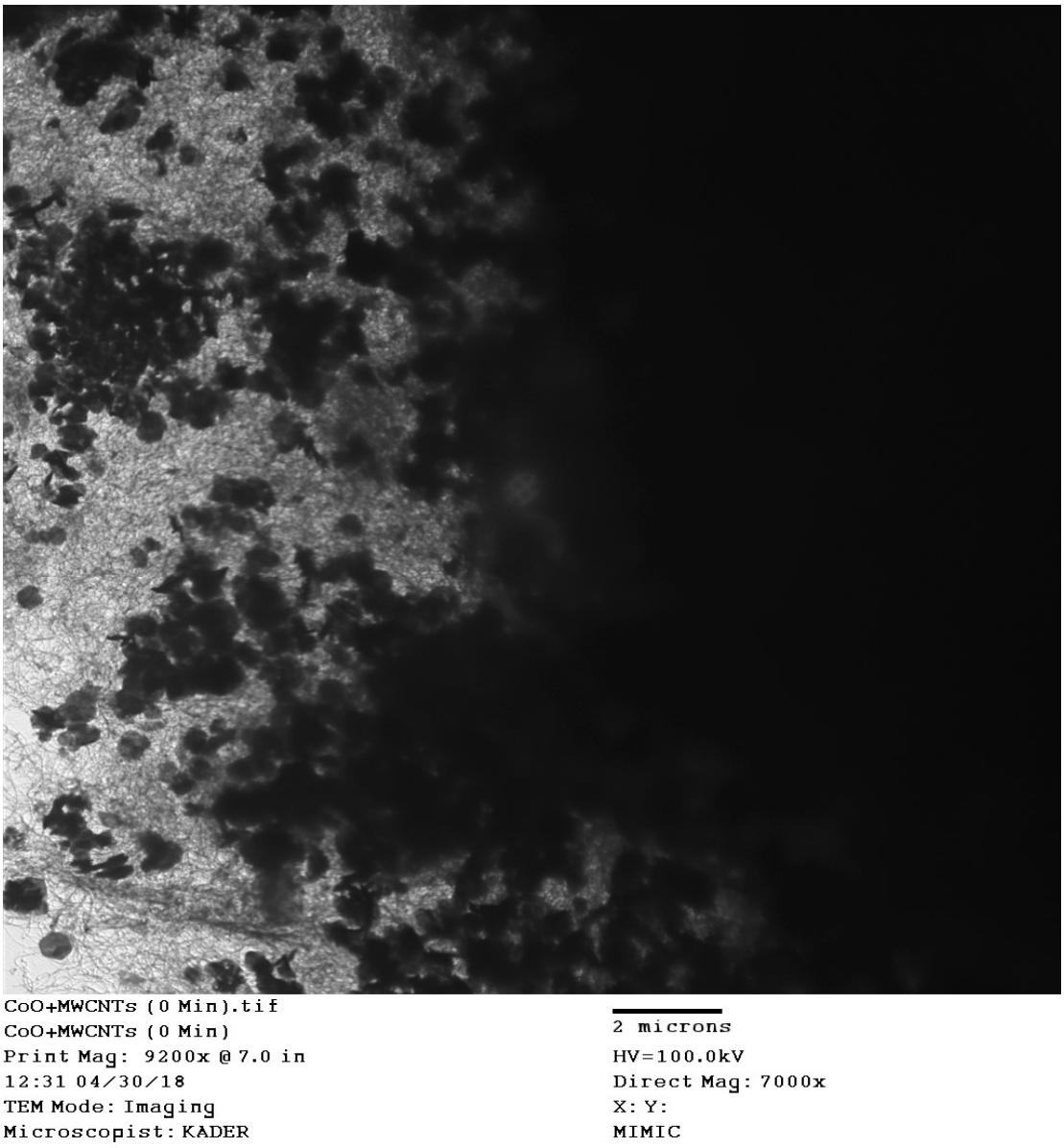

Figure 18: TEM images of CoO/COOH-MWNT composite in absolute anhydrous ethyl alcohol solution without sonication.

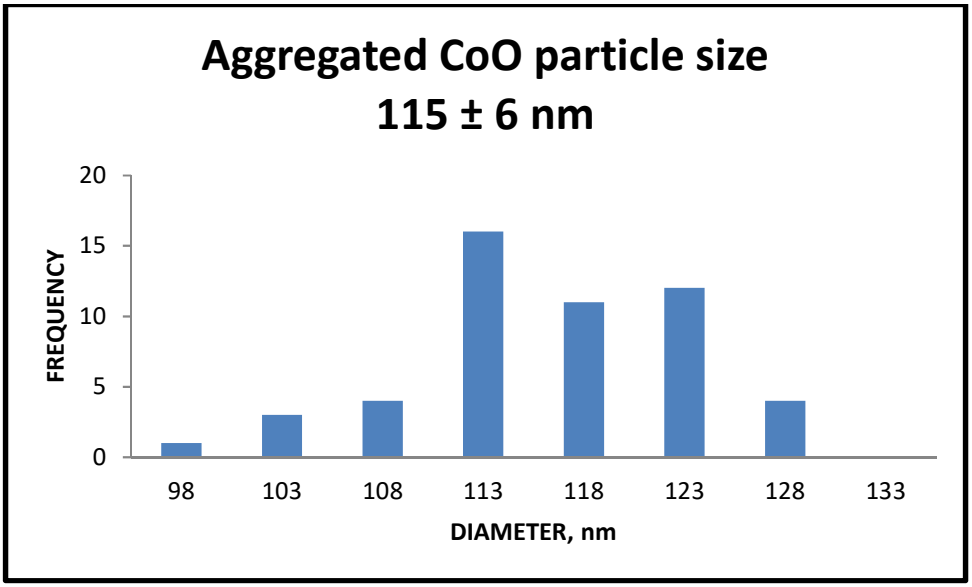

Figure 19: Size distribution histogram of CoO/COOH-MWNT composite without sonication.

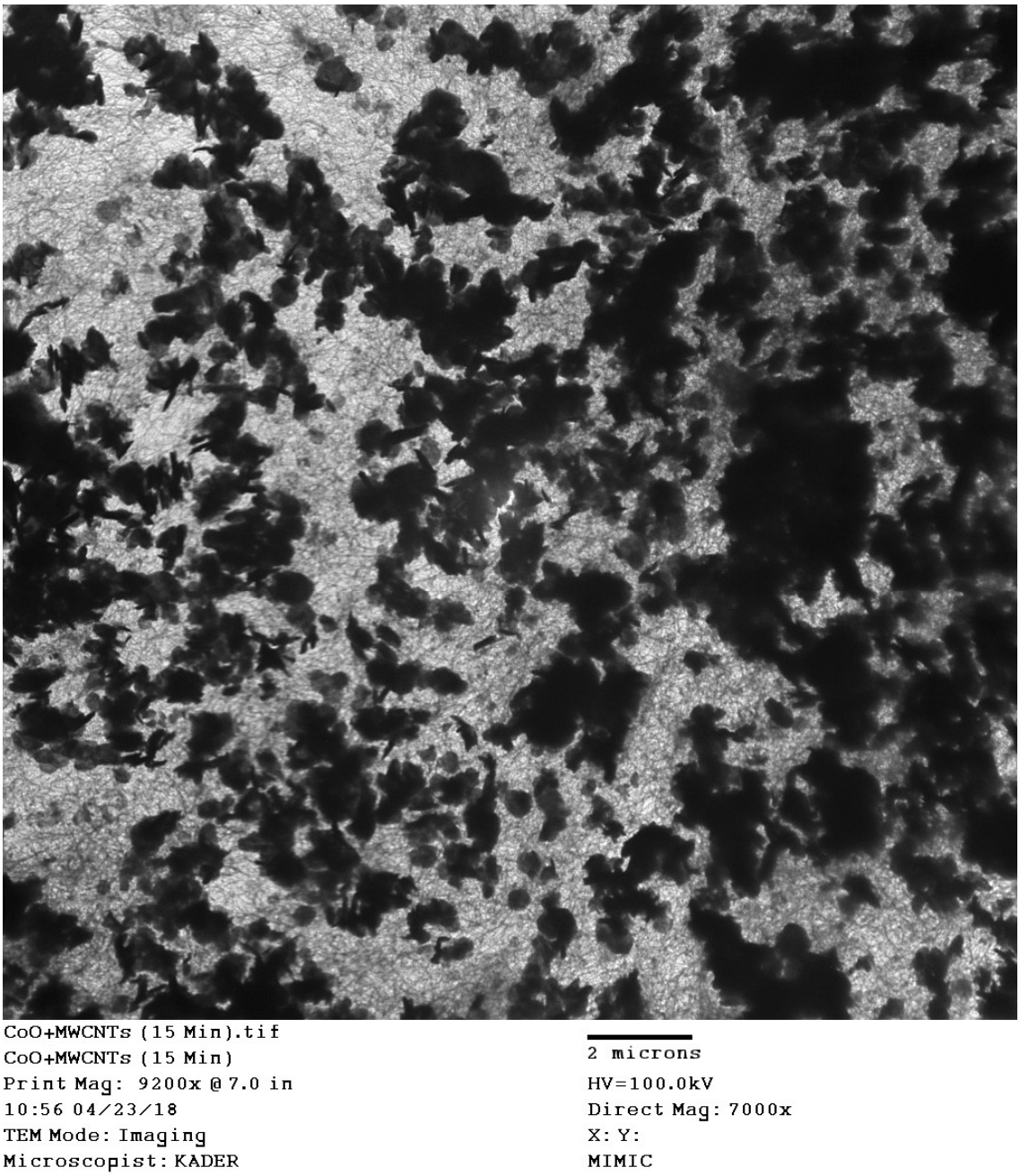

Figure 20: TEM images of CoO/COOH-MWNT composite in absolute anhydrous ethyl alcohol solution after a 15 min. sonication.

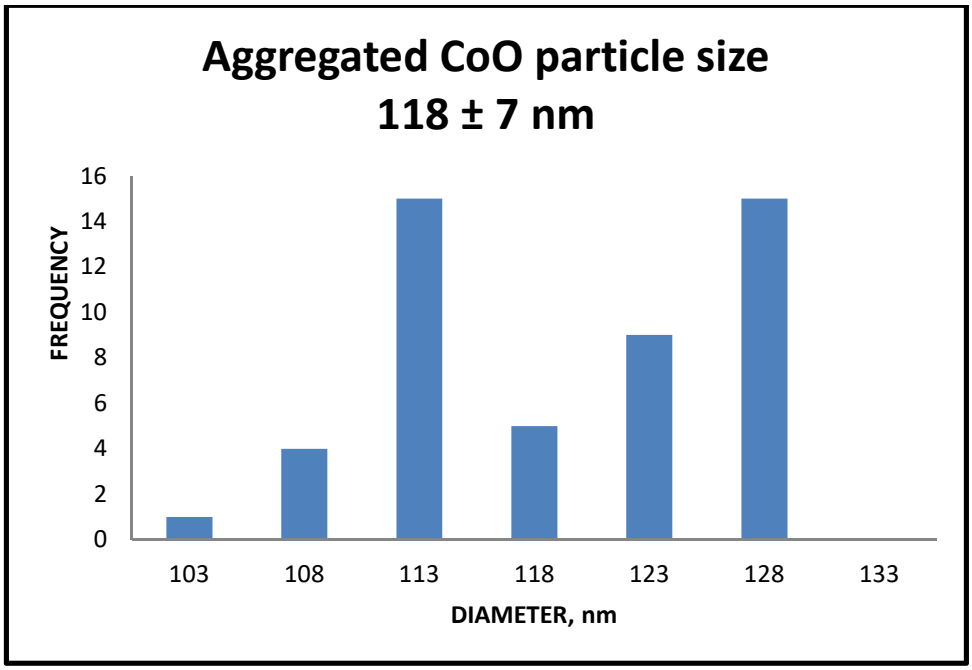

Figure 21: Size distribution histogram of 15 min. sonicated CoO/COOH-MWNT composite.

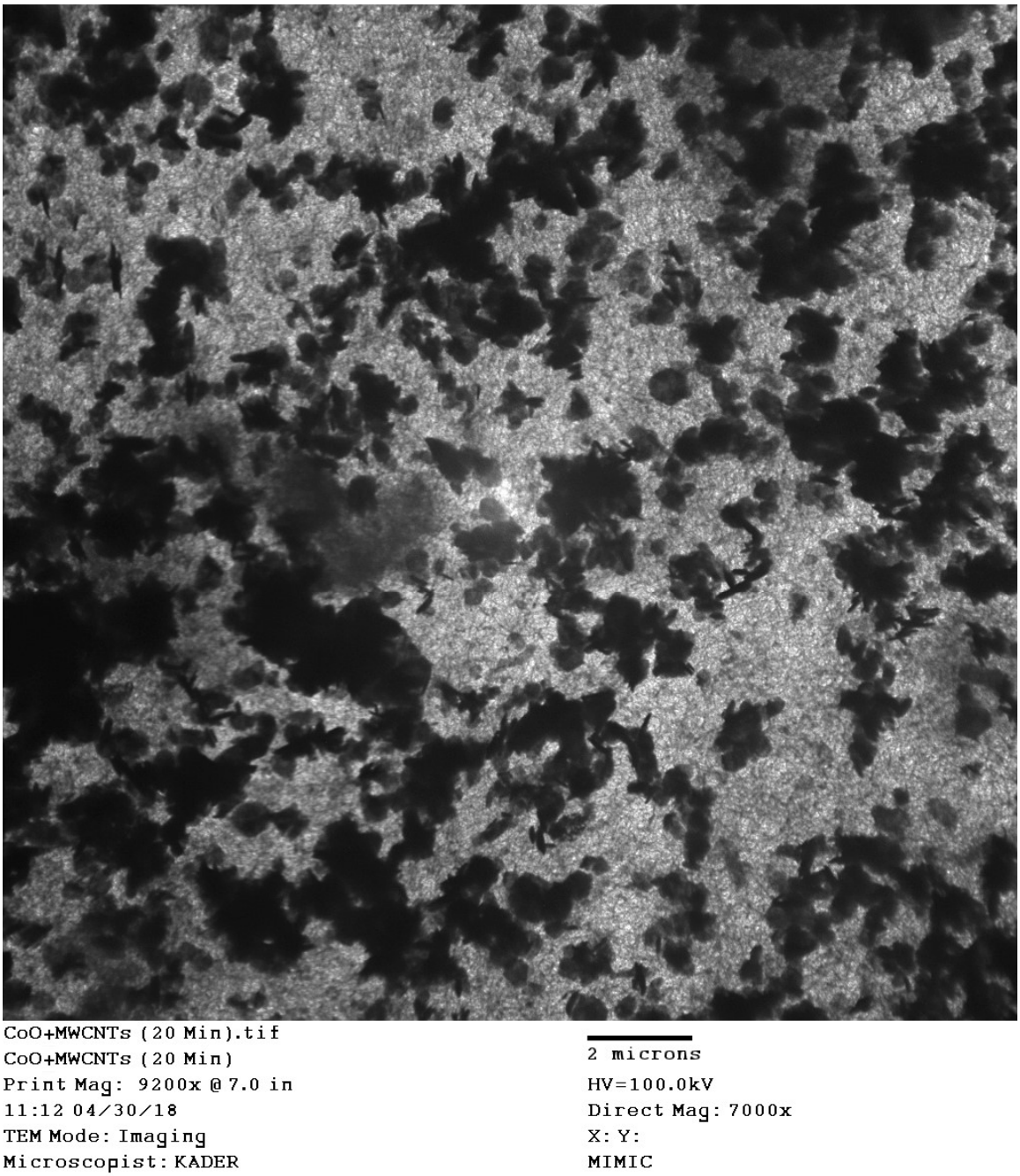

Figure 22: TEM images of CoO/COOH-MWNT composite in absolute anhydrous ethyl alcohol solution after a 20 min. sonication.

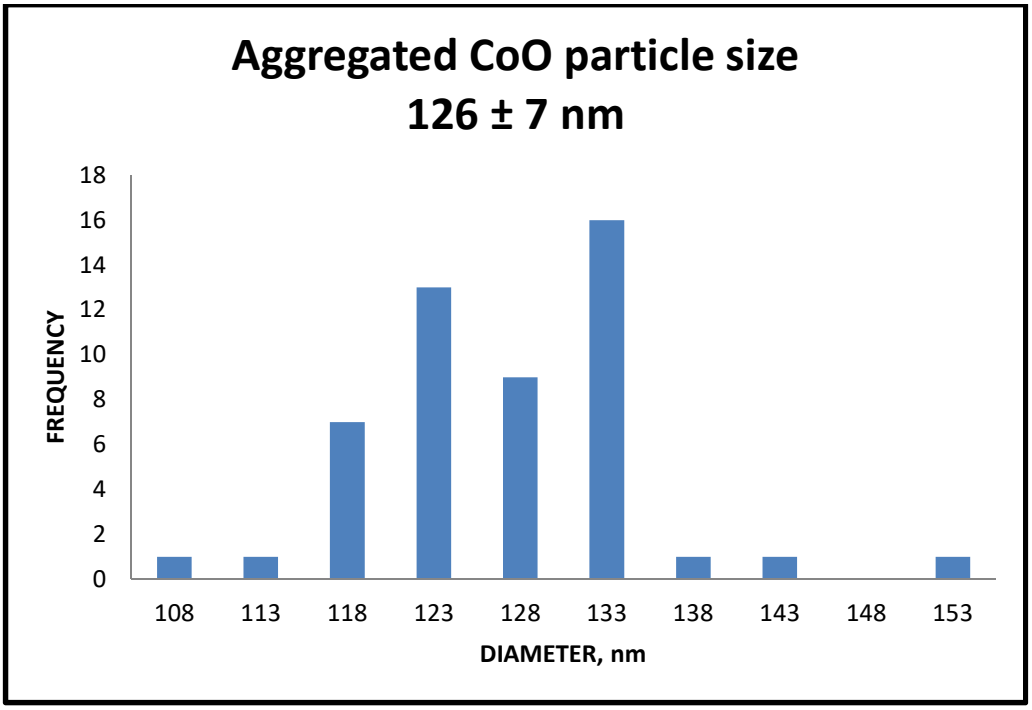

Figure 23: Size distribution histogram of 20 min sonicated CoO/COOH-MWNT composite.

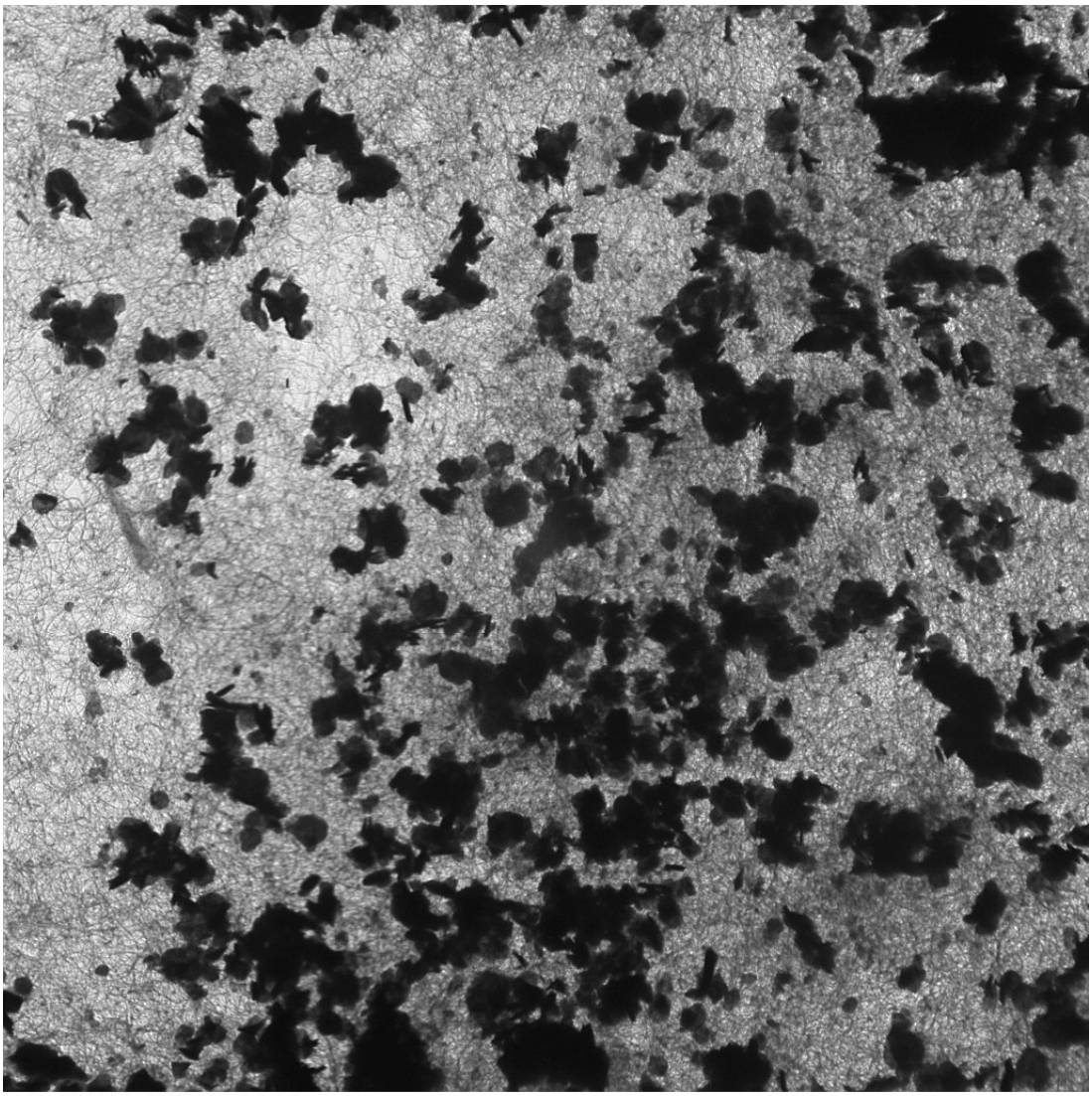

Figure 24: TEM images of CoO/COOH-MWNT composite in absolute anhydrous ethyl alcohol solution after a 30 min. sonication.

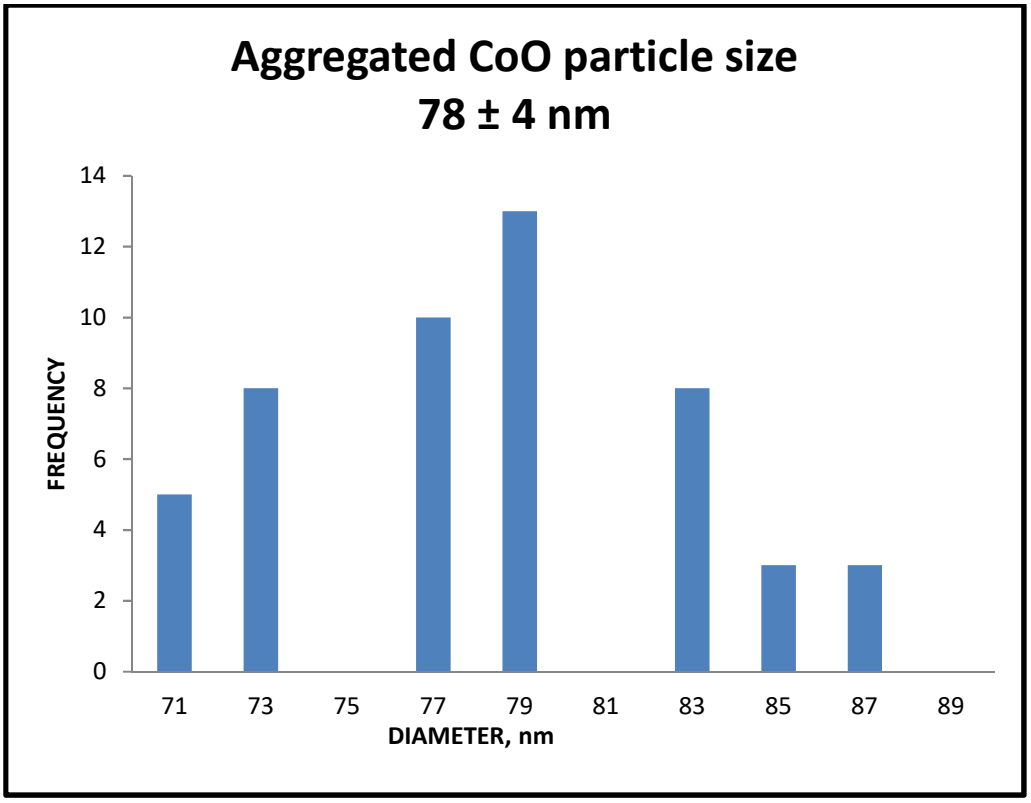

Figure 25: Size distribution histogram of 30 min. sonicated CoO/COOH-MWNT composite.

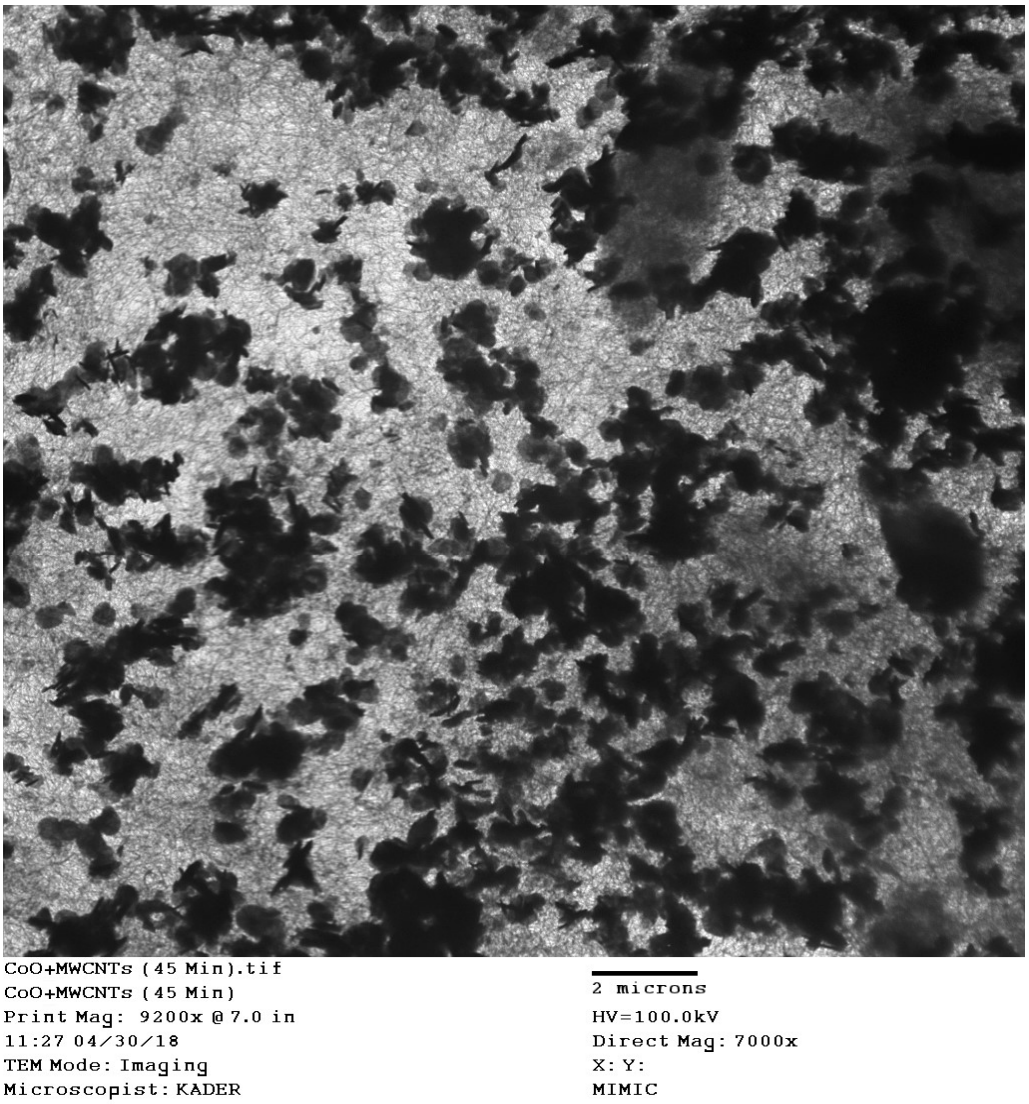

Figure 26: TEM images of CoO/COOH-MWNT composite in absolute anhydrous ethyl alcohol solution after a 45 min. sonication.

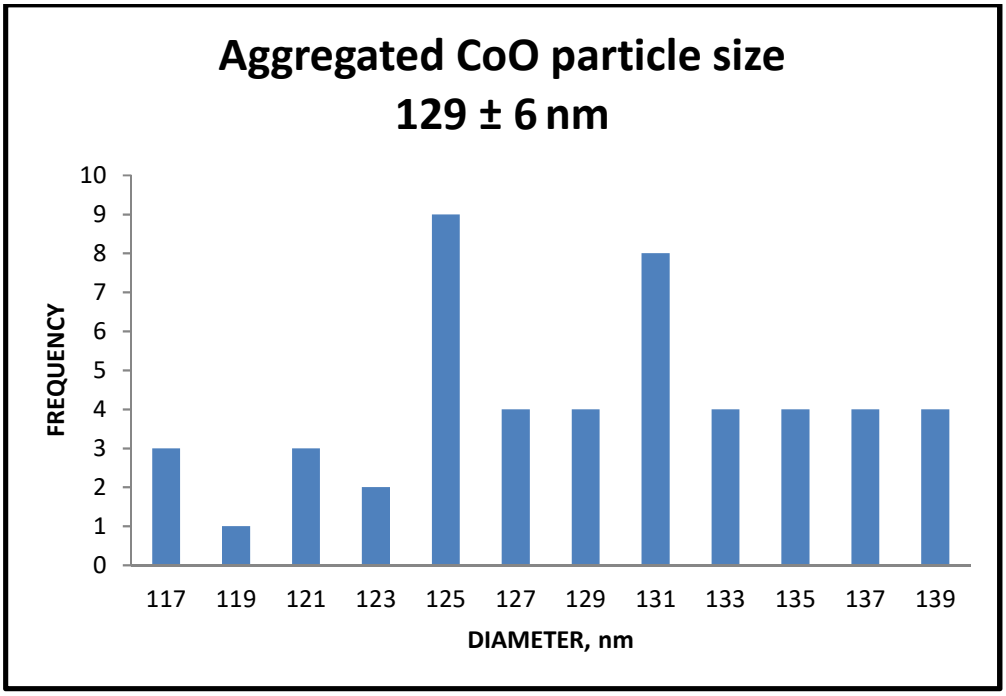

Figure 27: Size distribution histogram of 45 min. sonicated CoO/COOH-MWNT composite.

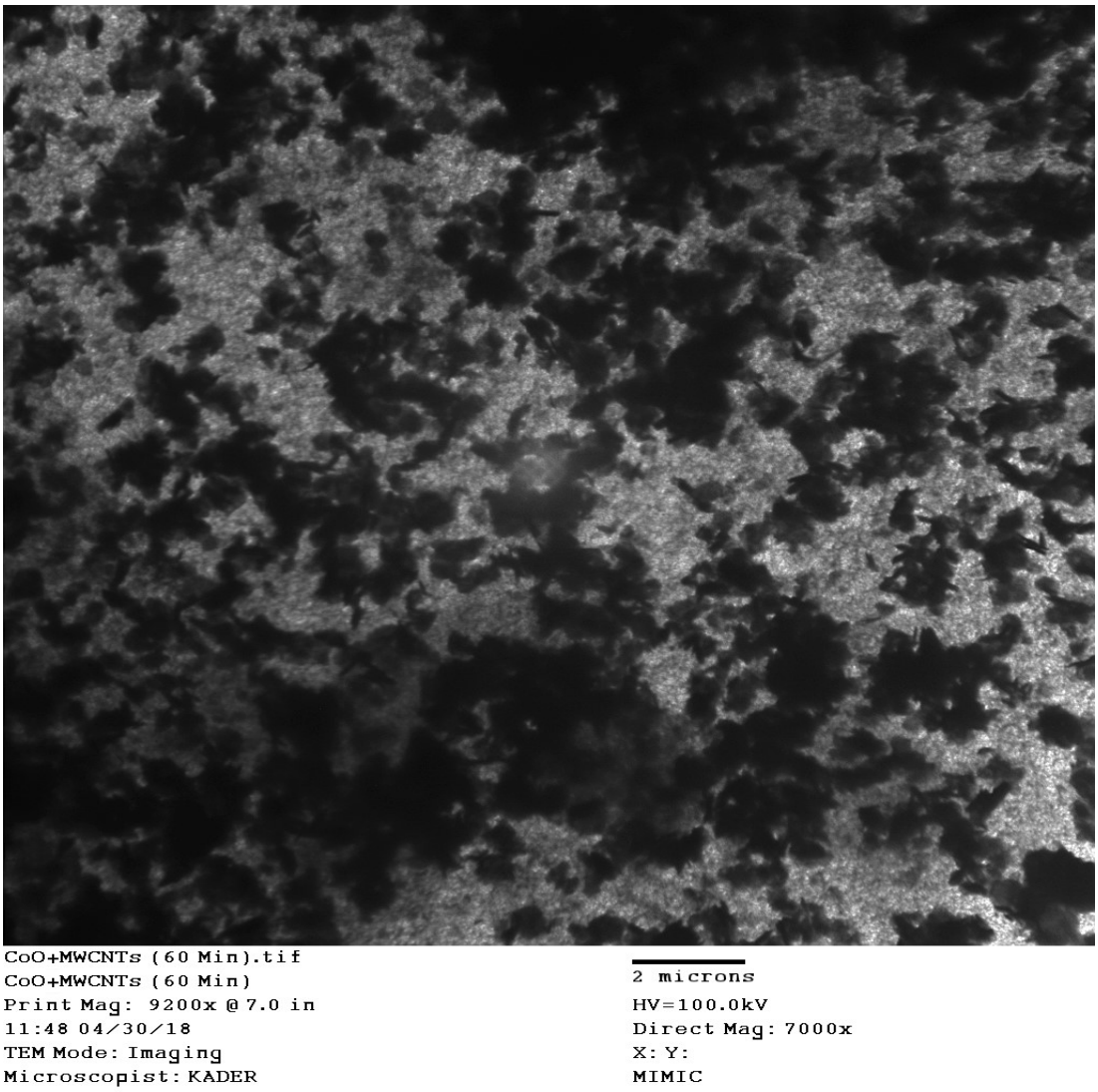

Figure 28: TEM images of CoO/COOH-MWNT composite in absolute anhydrous ethyl alcohol solution after a 60 min. sonication.

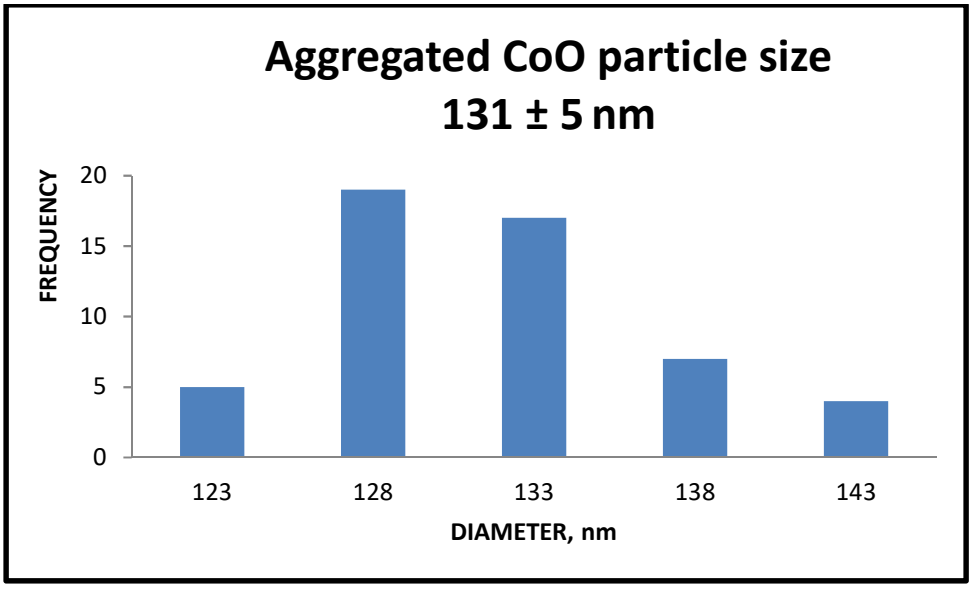

Figure 29: Size distribution histogram of 60 min. sonicated CoO/COOH-MWNT composite.

Figure 19, 21, 23, 25, 27 and 29 show size distribution histograms of CoO/COOH-MWNT at 0 (without sonication), 15, 20, 30, 45 and 60 min. sonication. At 0 min. sonication, Average aggregated CoO particle size is 115 ± 6 nm. Average aggregated CoO particle sizes found from the histograms 118 ± 7, 126 ± 7, 78 ± 4, 129 ± 6, 131 ± 5 nm consecutively at 15, 20, 30, 45 and 60 min. It is clear from study that the average particle size at 30 min. sonication time is the least than other sonication times. Also, from the TEM images, the average aggregated particle size distribution of the CoO/COOH-MWNT composite is maximum at 30 min. sonication. Due to the best distribution of CoO in COOH-MWNT, the composite showed maximum sensitivity at a 30 min. sonication towards dopamine detection.

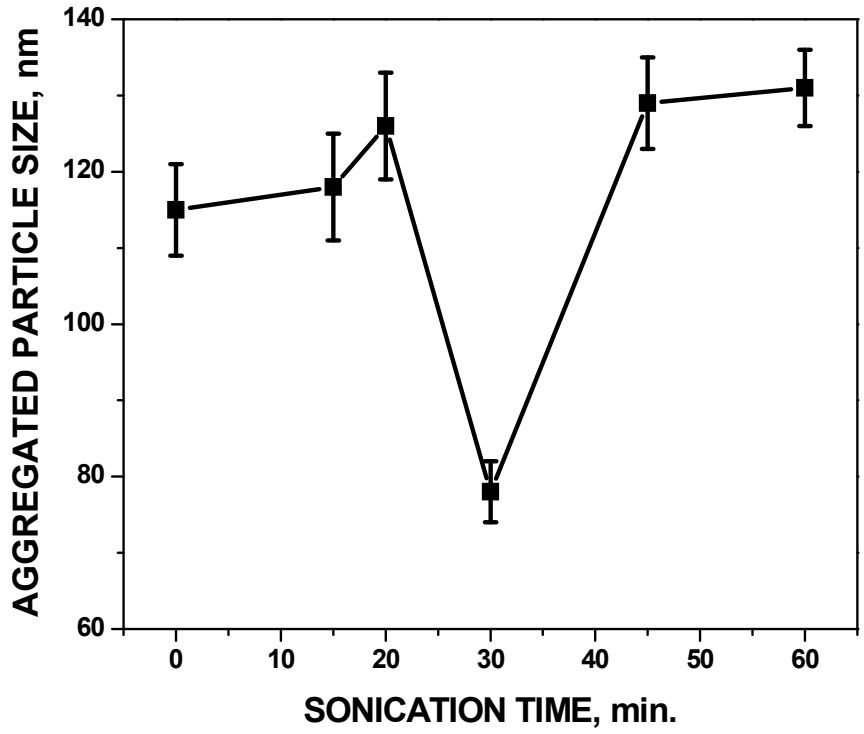

Figure 30: Plot of average aggregated particle size of CoO/COOH-MWNT vs sonication time.

Point-of- zero-charge (PZC) measurement of CoO/COOH-MWNT

The PZC is the pH of a solid surface which exhibits net zero charge at this pH. PZC is the concept of the pH at zero electrical charge density of a surface. The solid pH below PZC donates more protons and becomes positively charged. Due to the positive charge they attract anions and repeal cations. The PZC experiment in this thesis was done to study the best pH of the analyte solution to detect analytes by using the CoO/COOH-MWNT composite. The experiment was done according to Park and Regalbuto procedure.[45] **Figure 31** shows the plot of PZC measurements of CoO/COOH-MWNT composite. The PZC of CoO/COOH-MWNT composite was found 7.86. And best result was found to detect dopamine at pH 5.0 which is below PZC of the CoO/COOH-MWNT composite. Which indicates that the surface of the CoO/COOH-MWNT composite is positively charged. Negatively charged dopamine anions attracted by the positively charged composite surface. The attraction between positively charged surface and negatively charged anions can be explained by Coulombic attraction.

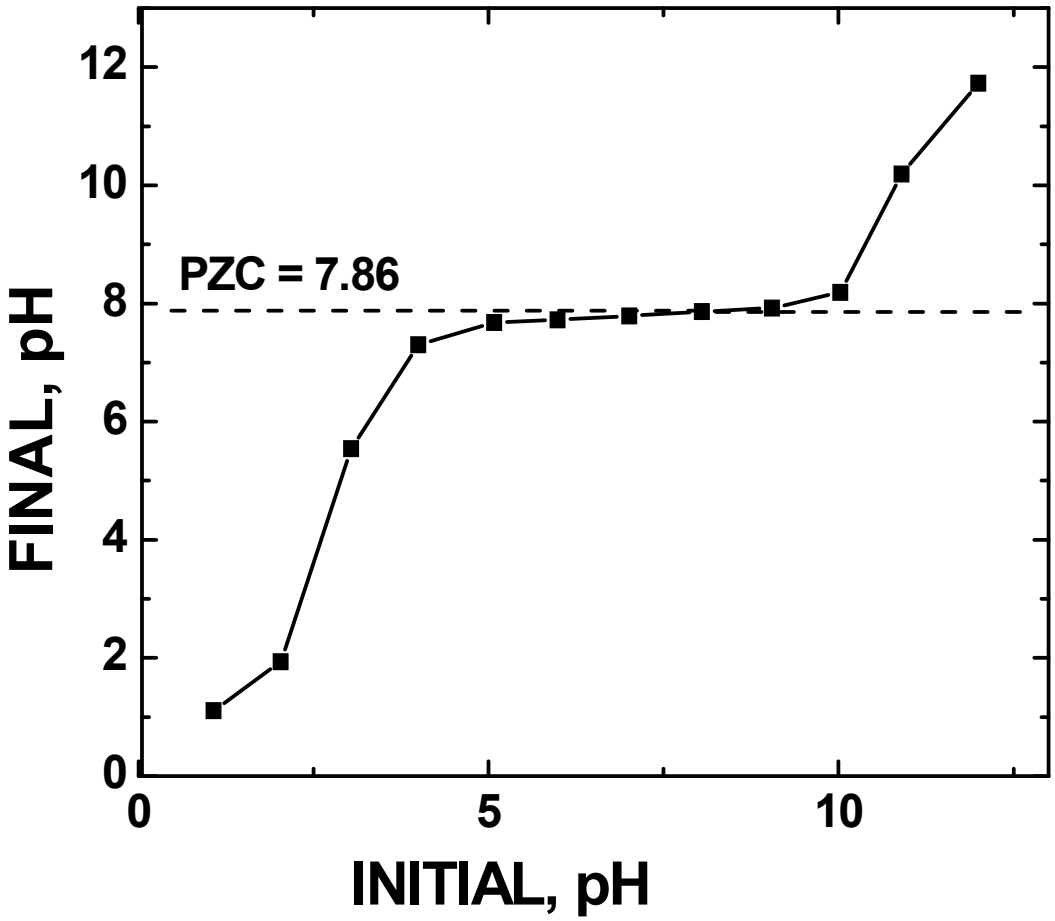

Figure 31: PZC plot of CoO/COOH-MWNT composite. The pH is 7.66 at PZC.

Electrocatalytic behavior of CoO/COOH-MWNT sensor

The electrocatalytic behavior of CoO/COOH-MWNT sensor was studied using cyclic voltammetry (CV). The composite shows excellent selectivity and sensitivity response toward the detection of DA.

Cyclic voltammetric (CV) experiment of dopamine

The Nafion/CoO/COOH-MWNT/GCE sensor acts as a working electrode in the electrochemical cell to perform CV experiments. **Figure 32** shows a typical cyclic voltammogram for 100 μM of dopamine. The voltammogram shows a sharp anodic peak at oxidation potential +0.3V. The sharp anodic peak indicates sensitivity of the CoO/COOH-MWNT/GCE sensor towards dopamine. N_2 gas was passed about 15 min. during CV experiments to provide an inert atmosphere inside the electrochemical cell in order to minimize other noise. The anodic peak due to the oxidation of dopamine will be seen within 0 to + 0.5V potential range during cyclic voltammetry experiments.

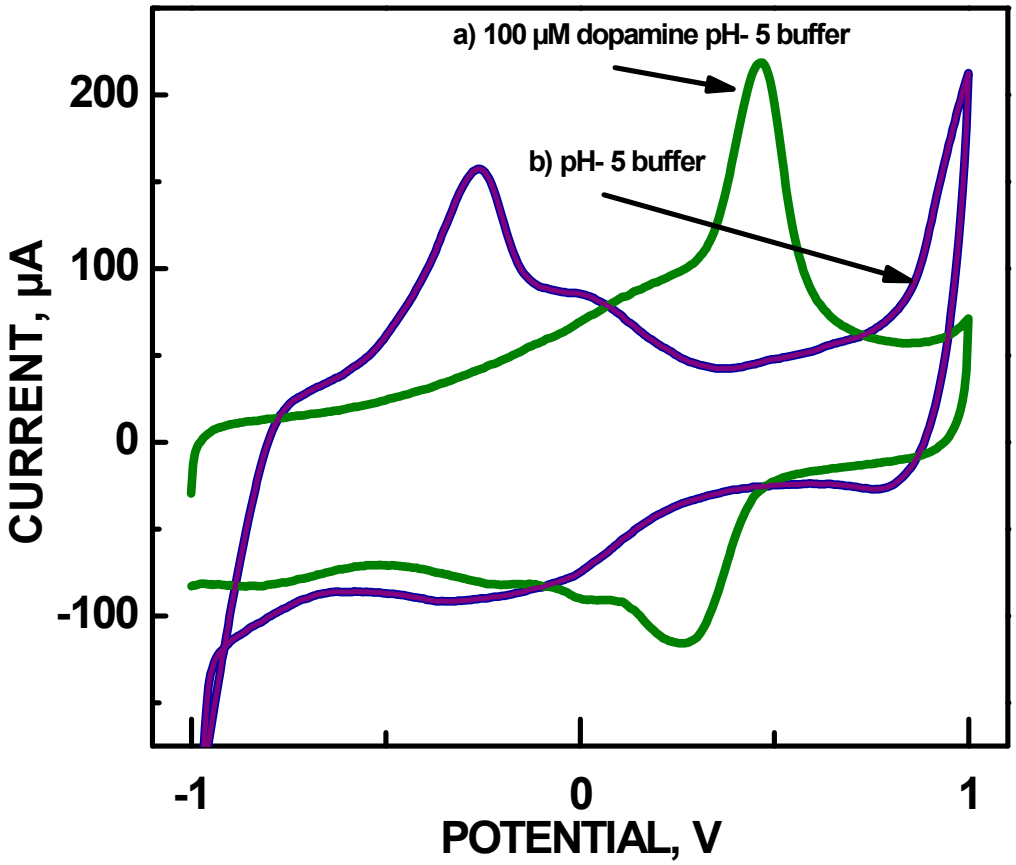

Figure 32: A typical cyclic voltammogram using CoO/COOH-MWNT/GCE electrochemical sensor a) at 100 µM dopamine at pH 5.0 buffer, and, b) pH 5.0 buffer only (control experiment).

Figure 33 shows cyclic voltammograms for dopamine using CoO/COOH-MWNT/GCE electrode, COOH-MWNT/GCE electrode, pure CoO /GCE electrode and blank GCE electrode. The modified CoO/COOH-MWNT/GCE electrode shows enhanced sensitivity towards dopamine compared to the other types of electrodes which are not modified by CoO particles.

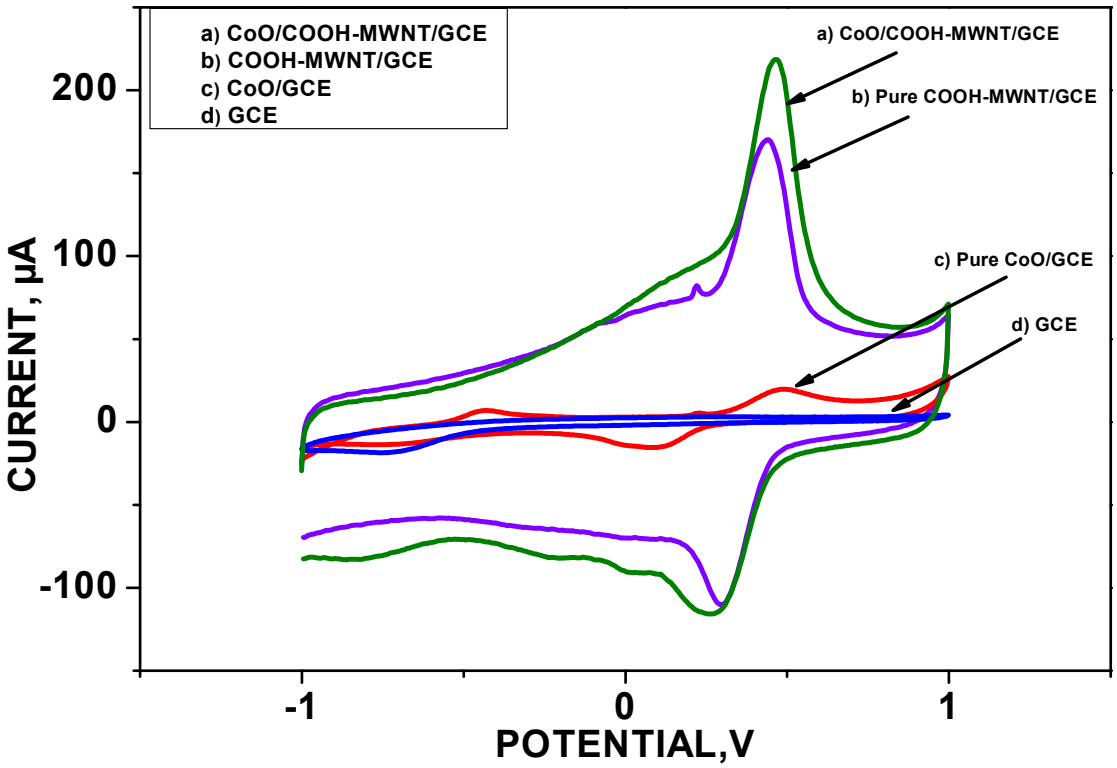

Figure 33: A typical cyclic voltammogram of 100 µM dopamine using a) CoO/COOH-MWNT /GCE, b) Pure COOH-MWNT/GCE, c) Pure CoO/GCE, and d) GCE.

The control study for the developed sensor was done using components of materials used in the modified composite. The study shows that the 2 wt % Nafion has no response towards dopamine and pure CoO and COOH-MWNT have low sensitivity with compared to the developed 2 wt % Nafion/CoO/COOH-MWNT composite.

Cyclic voltammetry experiments at different dopamine concentration using CoO/COOH-MWNT/GCE sensor

Figure 34 shows cyclic voltammogram for the different concentration of dopamine solutions using CoO/COOH-MWNT/GCE sensor. The concentration range of dopamine solutions is from 10 to 100 μM. The dopamine solutions were prepared by PBS, pH 7.0 (Sigma-Aldrich, St. Louis, MO, USA) and buffer solution pH 4.66 (EMD Millipore Corporation, Billerica, MA, USA). The current increases due to the increase of dopamine concentration. CoO/COOH-MWNT/GCE sensor shows maximum sensitivity towards 100 μM dopamine within 10 to 100 μM concentration range.

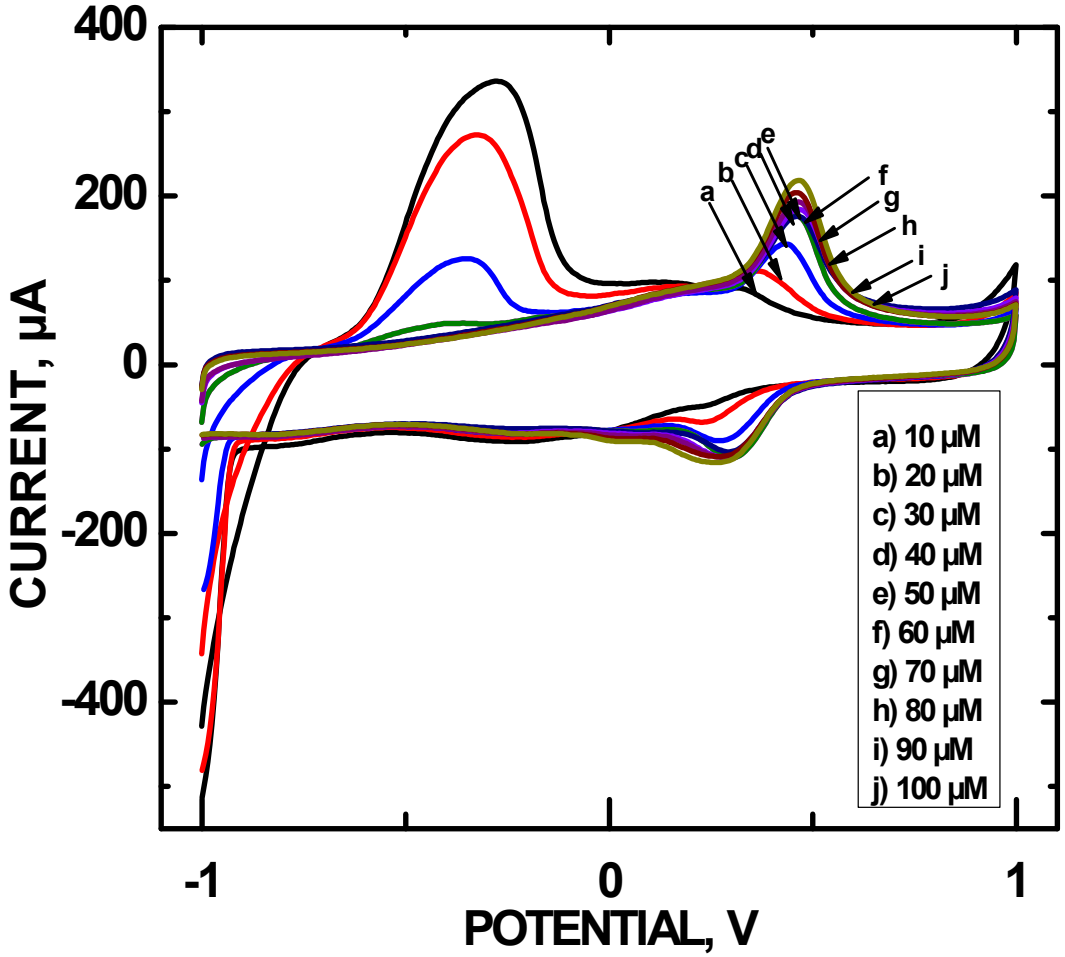

Figure 34: Cyclic voltammogram of various concentrations of dopamine solutions using Nafion /CoO/COOH-MWNT/GCE sensor in PBS at 0.3 V; in the concentration range of 10-100 µM dopamine.

Figure 35 is showing current versus dopamine concentration plot. There is a linear relationship at 10 to 100 µM dopamine concentration. Here, I_{PC} = 1.45738 [dopamine] µM + 6.1843 with correlation coefficient (R^2) of 0.9522.

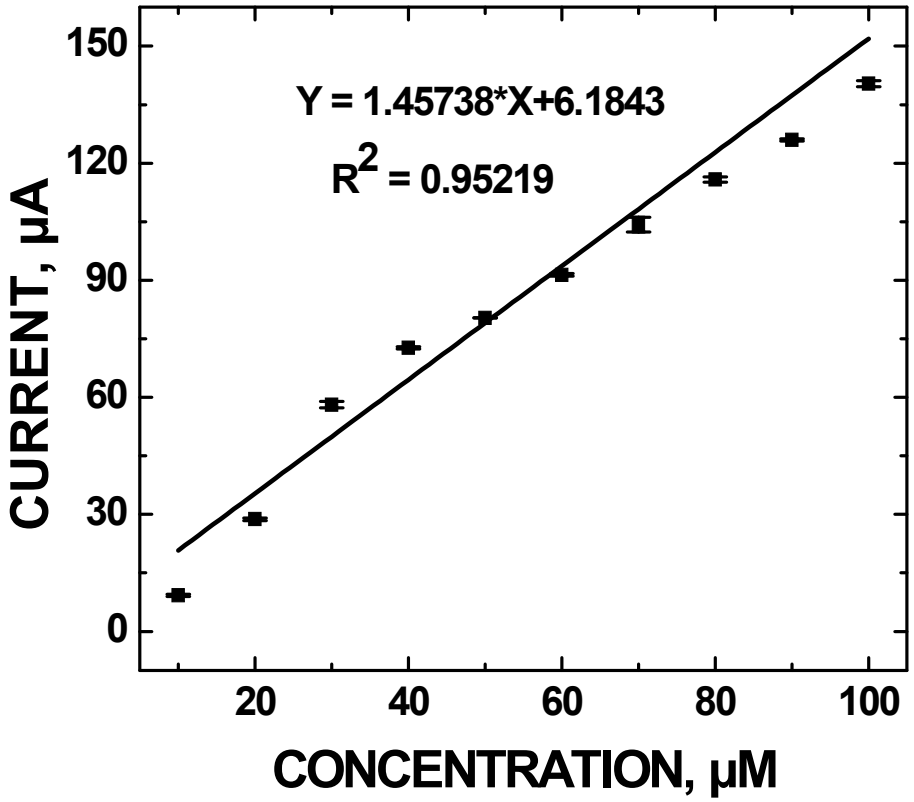

Figure 35: Current versus dopamine concentration plot.

Figure 36 shows cyclic voltammogram for the 0.5 to 5.0 µM concentration of dopamine using CoO/COOH-MWNT/GCE sensor.

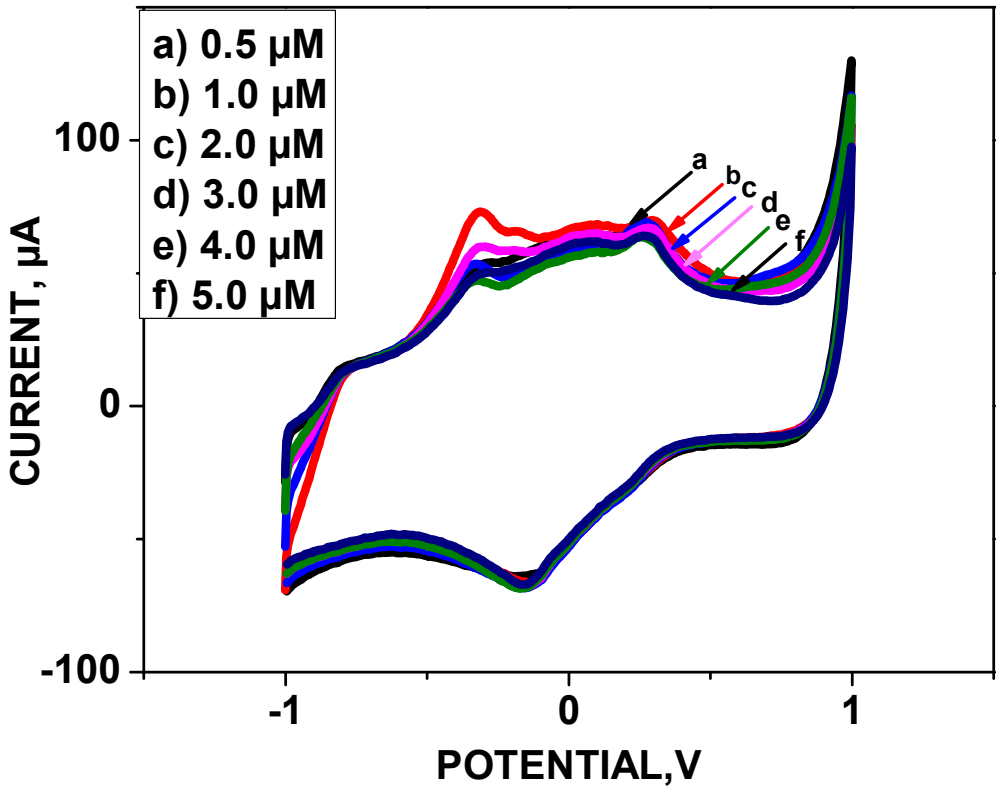

Figure 36: CV study using Nafion /CoO/COOH-MWNT /GCE

at 0.3 V; in the concentration range of (0.5-5) µM dopamine.

Figure 37 is showing, current versus dopamine concentration plot. There is a quadratic relationship at (0.5-5.0) µM dopamine concentration.

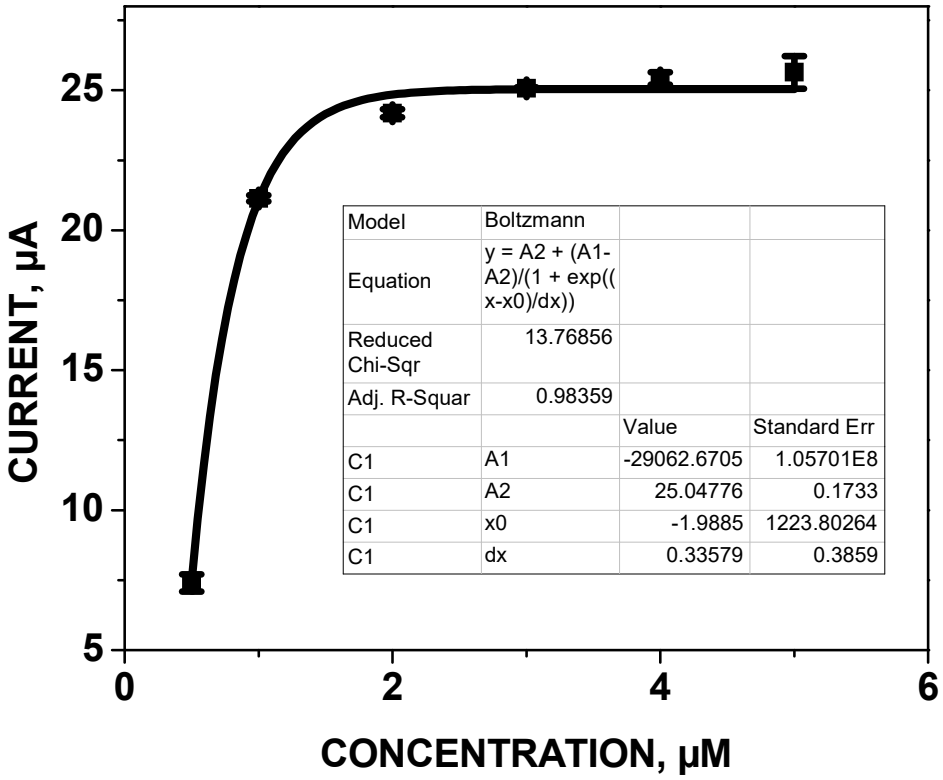

Figure 37: Current versus dopamine concentration plot.

.

Cyclic voltammetry experiment at different loading of CoO/COOH-MWNT composite

Figure 38 shows cyclic voltammogram for a sequence of different loadings of composite (CoO/COOH-MWNT) with dopamine concentration of 100 µM. The current is increasing with the variation of composite loading.

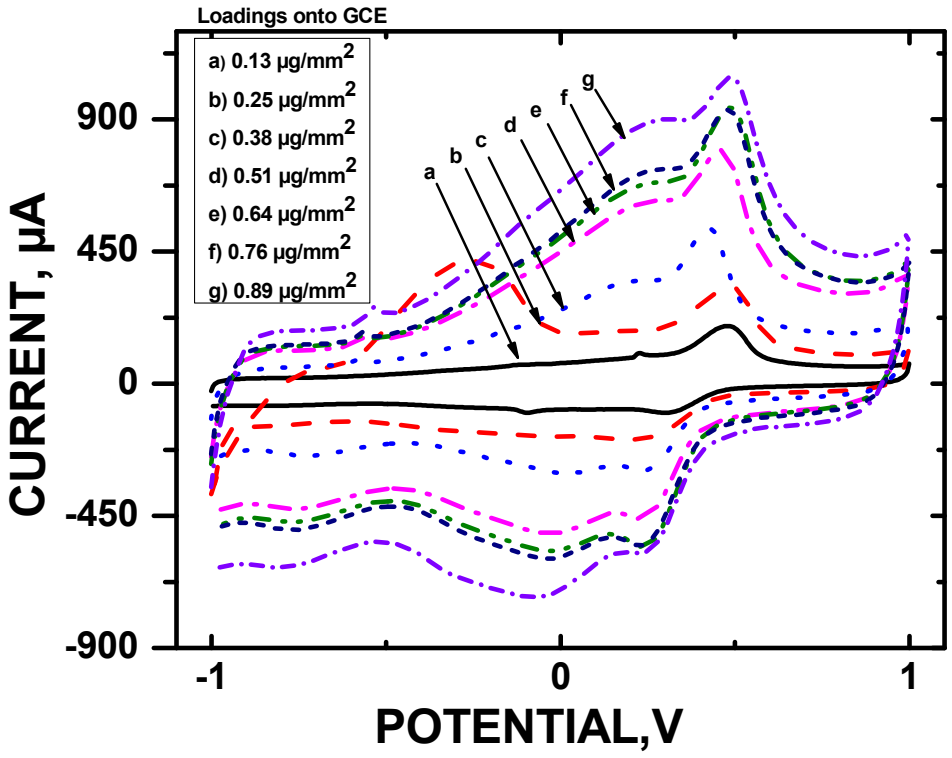

Figure 38: Cyclic voltammograms for dopamine at (a) 0.13 µg/mm^2, (b) 0.25 µg/mm^2, (c) 0.38 µg/mm^2, (d) 0.51 µg/mm^2, (e) 0.64 µg/mm^2, (f) 0.76 µg/mm^2, (g) 0.89 µg/mm^2 loadings of the CoO/COOH-MWNT/GCE composite in PBS at pH 7.0 under N_2 atmosphere.

Cyclic voltammetry experiment of dopamine solution at various pH

Figure 39 shows cyclic voltammograms for different pH of buffer solution with dopamine concentration of 100 µM. The voltammogram shows a nonlinear relationship in peak current with the change of pH. The maximum sensitivity was found at pH 5.0.

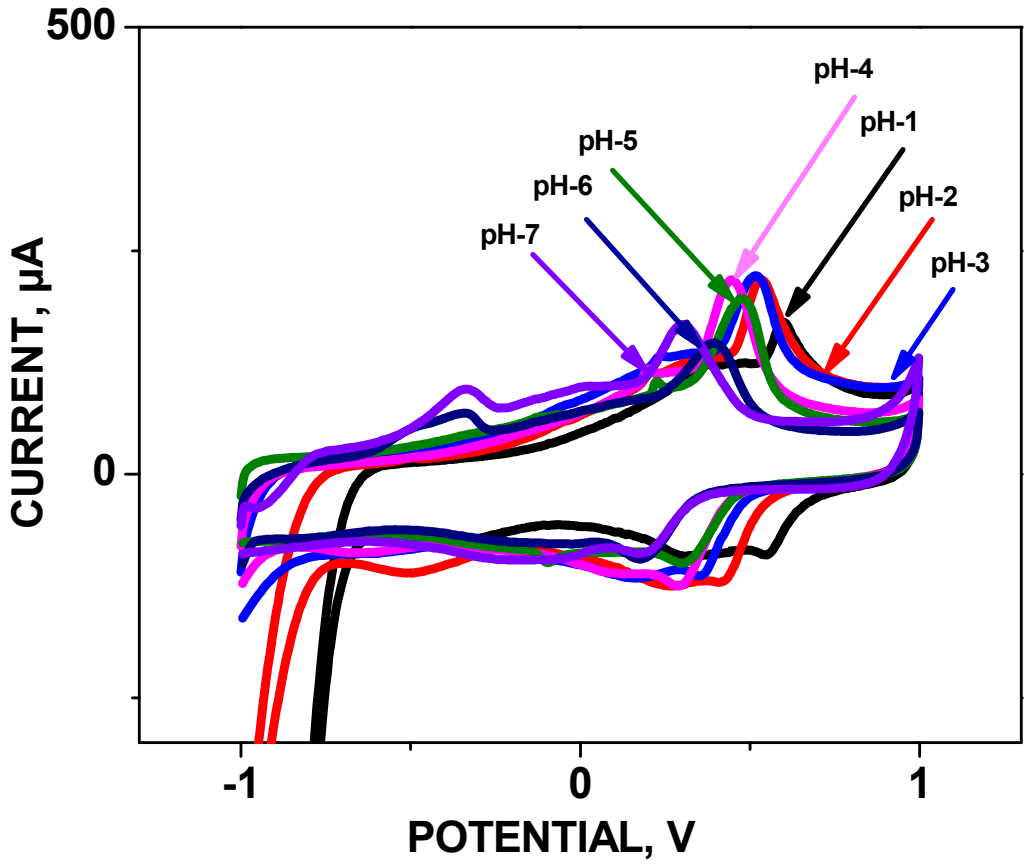

Figure 39: A typical cyclic voltammogram of 100 µM dopamine using Nafion/CoO/COOH-MWNT/GCE at various pH solution.

Figure 40 is showing current versus pH plot at 1-7 pH range for 100 µM dopamine.

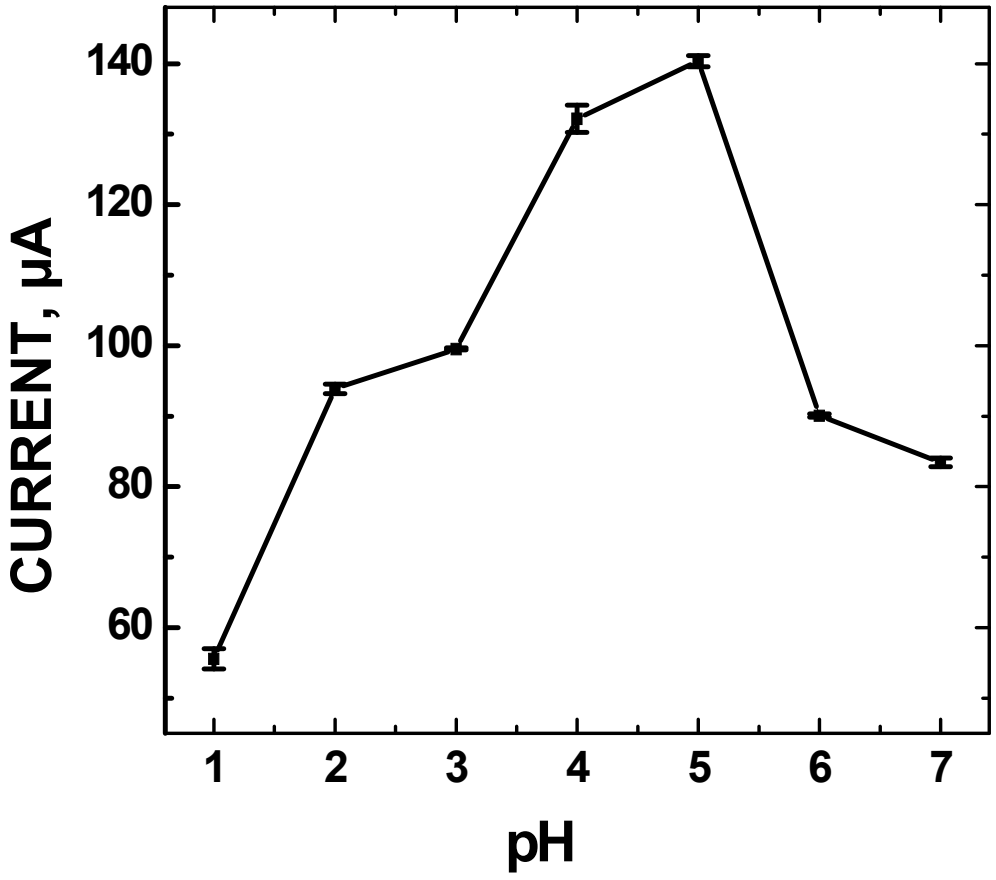

Figure 40: Peak current versus pH of 100 µM dopamine.

.

Cyclic voltammetry experiment of dopamine solution at various sonication times

Figure 41 shows CVs for composites produced at various sonication times with dopamine concentration of 100 µM. The maximum sensitivity was found at a 30 min. sonication time.

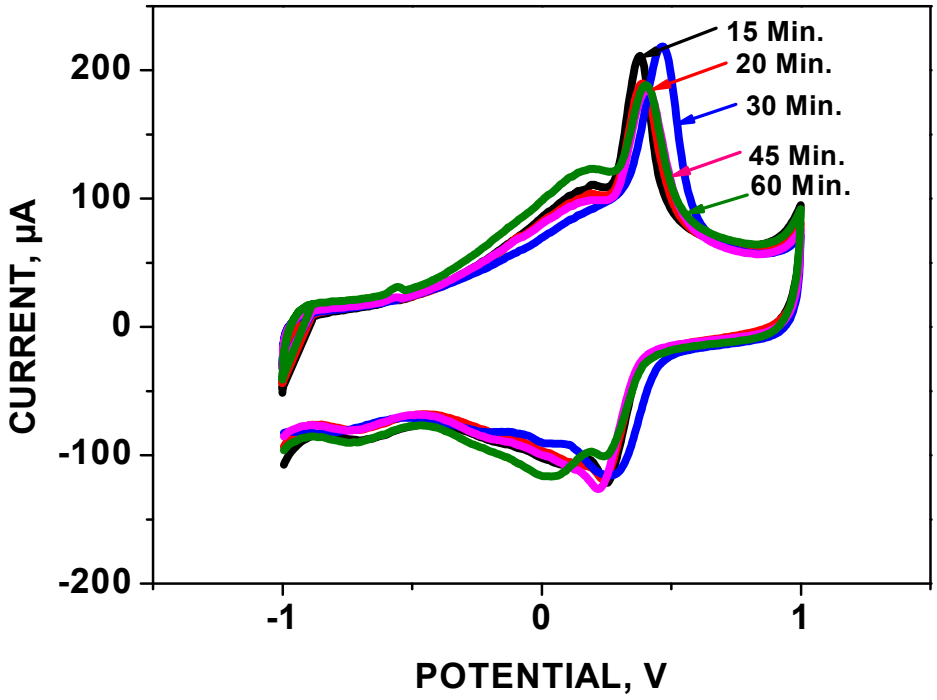

Figure 41: A typical cyclic voltammogram of 100 µM dopamine using Nafion /CoO/COOH-MWNT/GCE at different sonication times.

Figure 42 shows a plot of peak current versus sonication time ranging from 15 to 60 min.

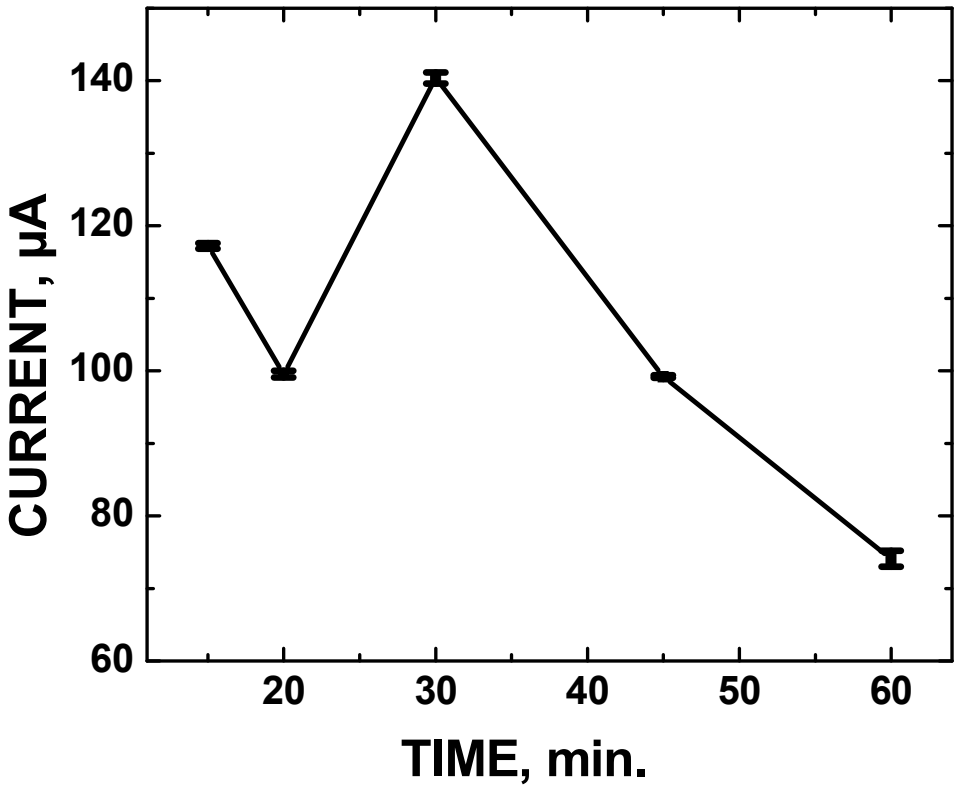

Figure 42: Peak current versus sonication time.

Selectivity study of CoO/COOH-MWNT/GCE electrochemical sensor toward dopamine

The Nafion/CoO/COOH-MWNT/GCE electrochemical sensor is selective toward dopamine. **Figure 43** shows that the sensor can only detect dopamine. It has no response towards ascorbic acid and uric acid.

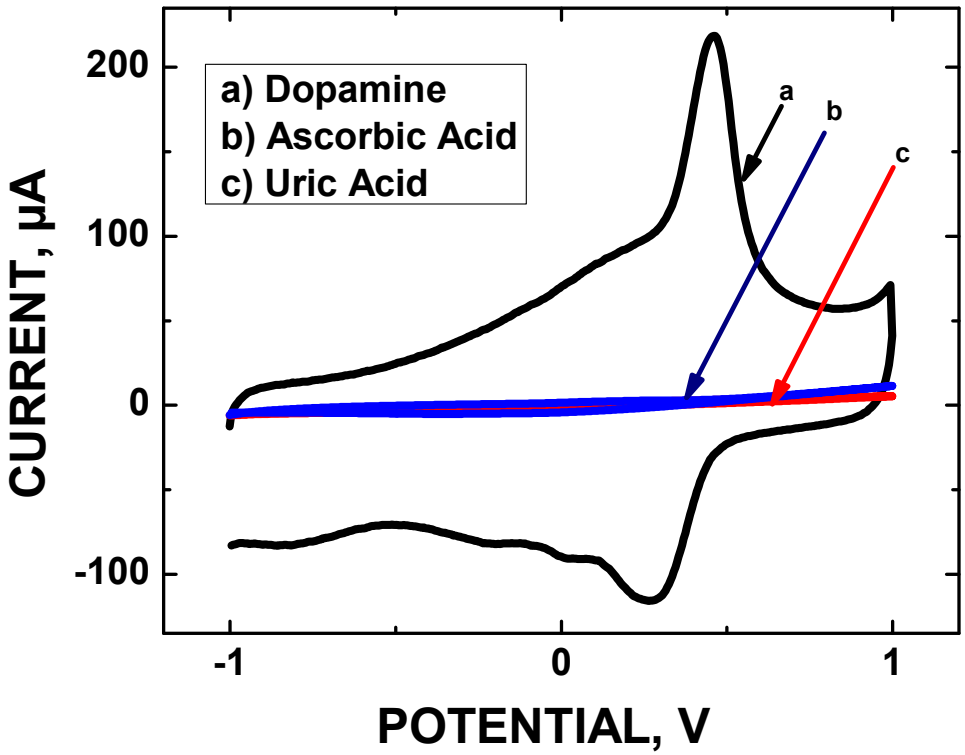

Figure 43: Peak current versus sonication time plot showing selectivity of the Nafion/CoO/COOH-MWNT/GCE electrochemical sensor towards 100 µM dopamine.

CHAPTER IV

CONCLUSION

The developed CoO/COOH-MWNT electrochemical sensor showed excellent sensitivity and selectivity towards the detection of dopamine. The sensitivity was studied by cyclic voltammetry experiments. Elemental and optical characterization was done by ATR-IR, Raman spectroscopy, XPS, and TEM experiments. The minimum detection limit of dopamine using CoO/COOH-MWNT sensor was found 0.5 μM. The plot of peak current vs dopamine concentration showed linear relationship at 10-100 μM range. The linear relationship indicates that the electrochemical reactions at 10-100 μM range are diffusion controlled. The plot of peak current vs dopamine concentration showed quadratic relationship at 0.5-5.0 μM range. Therefore, the quadratic relationship indicates that the electrochemical reactions at 0.5-5.0 μM range are kinetically controlled. The sensor showed maximum sensitivity towards dopamine at 30 min. sonication time. Raman study, ATR-IR and TEM study supports this finding. The D-to-G peak integrated area ratio was found 2.59, which is maximum compare to other sonication time. The maximum D-to-G peak integrated area ratio indicates the presence of maximum disordered sp^3 hybridized carbon. The ATR-IR study showed the attachment of CoO particles with COOH-MWNT at 30 min. sonication. Also, TEM experiments show that average aggregated particle size at 30 min. sonication is 78 ± 4 nm, which is smaller average particle size with compare to other sonication time. The maximum sensitivity of

the sensor was also found for 0.89 μg/mm^2 loading of composite and pH 5.0 buffer solutions during cyclic voltammetry experiments. The XPS study showed the atomic percentage at top most surface of the CoO/COOH-MWNT composite. 97.03% C 1s, 2.83% O 1s and 0.14% Co 2p was found from XPS analysis. The spin orbit coupling of Co 2p was found 15.9 eV. from Co 2p peak, which is the characteristic of CoO.

The presence of ascorbic acid (AA) and uric acid (UA) interfere with the dopamine (DA) during electrochemical detection of dopamine and electrochemical approach becomes difficult.[46-51] The CoO/COOH-MWNT/GCE sensor showed no response towards AA and UA. During this thesis project, we tried to develop a simple and inexpensive method to detect dopamine with good selectivity for regular analysis. The developed CoO/COOH-MWNT/GCE sensor showed fast electrochemical response with good sensitivity and selectivity to dopamine with complete elimination of interferences from AA and UA.

REFERENCES

1. Vollath, D., *Nanomaterials: An Introduction to Synthesis, Properties and Application,* Wiley-VCH Verlag GmbH & Co.; Weinheim, Germany, **2008**, Vol. 7, pp 865-870.
2. Lue, J. T., *Physical properties of nanomaterials*, Encyclopedia of Nanoscience and Nanotechnology, **2007**, Vol. X, pp 1–46.
3. Sajanlal, P.R.; Sreeprasad, T. S.; Samal, A. K.; Pradeep, T., Anisotropic nanomaterials: structure, growth, assembly, and functions, *Nano Reviews*, **2011**, Vol. 2, pp 1-62.
4. Sabaeian, M.; Khaledi-Nasab, A., Size-dependent intersubband optical properties of dome-shaped InAs/GaAs quantum dots with wetting layer, *Applied Optics*, **2012**, 51, 4176-4185.
5. Elham, A.; Aval, S. F.; Akbarzadeh, A.; Milani, M.; Nasrabadi, F. T.; Joo, S. W.; Hanifehpour, Y.; Nejati-Koshki, K.; Pashaei-Asi, R., Dendrimers: Synthesis, Applications, and Properties, *Nanoscale Res Lett.,* **2014**, 9, 247.
6. Wang, X.; Li, Q.; Xie, J.; Jin, Z.; Wang, J.; Li, Y.; Jiang, K.; Fan, S., Fabrication of Ultralong and Electrically Uniform Single-Walled Carbon Nanotubes on Clean Substrates, *Nano Letters*, **2009**, 9, 3137–3141.
7. Kaushik; Brajesh, K.; Majumder; Kumar, M., Carbon Nanotubes Based VSLI Interconnects, *Springer Briefs in Applied Sciences and Technology,* **2015**, 1, 17-37.
8. Mukul, K.; Ando, Yoshinori, A., Chemical vapor deposition of carbon nanotubes: A review on growth mechanism and mass production, *Journal of Nanoscience and Nanotechnology*, **2010**, 10, 3739-3758.

9. Zhang, M.; Li, J., Carbon nanotube in different shapes, *Materials today,* **2009**, 12, 12-18.
10. Eatemadi, A.; Daraee, H.; Karimkhanloo, H.; Kouhi, M.; Zarghami, N.; Akbarzadeh, A.; Abasi, M.; Hanifehpour, Y.; Joo, S. W., Carbon nanotubes: Properties, synthesis, purification, and medical applications, *Nanoscale Res Lett.,* **2014**, 9, 393.
11. Pantano, A., *Carbon Nanotube Based Composites: Processing, Properties, Modelling and Application,* Smithers Rapra, UK, 2012, 1-42.
12. Cheung, W.; Pontoriero, F.; Taratula, O.; Chen, A. M.; He, H., DNA and carbon nanotubes as medicine, *Advanced Drug Delivery Reviews,* **2010**, 62, 633-649.
13. Sabarinath, B.; Elangovan, P., Storage of sun's heat by using modified carbon nanotubes, *Nanoscience, Engineering and Technology (ICONSET)*, **2011**, 1, 437-440.
14. Zavalniuk, V.; Marchenko, S., Theoretical analysis of telescopic oscillations in multi-walled carbon nanotubes, *Low Temperature Physics*, **2011**, 37, 337-338.
15. Bonard, J.; Maiera, F.; Stöckli, T.; Châtelain, A.; Heer, W.; Salvetat, J.; Forróc, L., Field emission properties of multiwalled carbon nanotubes, *Ultramicroscopy*, **1998,** 73, 7-15.
16. Fang, B.; Zhang, C.; Zhang, W.; Wang, G., A novel hydrazine electrochemical sensor based on a carbon nanotubes-wired ZnO nanoflowers-modified electrode, *Electrochim. Acta,* **2009**, *55*, 178-182.
17. Hirsch, A.; Vostrowsky, O., *Functional Molecular Nanostructures,* Springer, Berlin, Heidelberg, **2005**, 193-237.
18. Jeon, I.; Chang, D. W.; Kumar, N. A.; Baek, J. B., *Functionalization of Carbon Nanotubes*, InTech, **2011**, 9-21.

19. Vardharajula, S.; Ali, S. Z.; Tiwari, P. M.; Eroğlu, E.; Vig, K.; Dennis, V. A.; Singh, S. R., Functionalized carbon nanotubes: biomedical applications, *Int J Nanomedicine*, **2012**, 7, 5361–5374.

20. Mauro, M.; Crosera, M.; Pelin, M.; Florio, C.; Bellomo, F.; Adami, G.; Apostoli, P.; Palma, G. D.; Bovenzi, M.; Campanini, M.; Filon, F. L., Cobalt Oxide Nanoparticles: Behavior towards Intact and Impaired Human Skin and Keratinocytes Toxicity, *Int J Environ Res Public Health*, **2015**, 12, 8263–8280.

21. Ahmed, J.; Ramanujachary, K. V.; Lofland, S. E.; Ganguli, A. K., Development of a microemulsion-based process for synthesis of cobalt (Co) and cobalt oxide (Co_3O_4) nanoparticles from submicrometer rods of cobalt oxalate, *J Colloid Interface Sci.*, **2008**, 321, 434-441.

22. Lang, J.; Yan, X.; Xue, Q., Facile preparation and electrochemical characterization of cobalt oxide/multi-walled carbon nanotube composites for supercapacitors, *Journal of Power Sources*, **2011**, 196, 18, 7841-7846.

23. Jiang, L.; Nelson, G. W.; Abda, J.; Foord, J. S., Novel modifications to carbon-based electrodes to improve the Electrochemical Detection of dopamine, *ACS Appl. Mater. Interfaces,* **2016**, 8, 28338-28348.

24. Zhao, J.; Zhang, W.; Sherrell, P.; Razal, J. M.; Huang, X.; Andrew I.; Minett, A. I.; Jun, C., Carbon Nanotube Nanoweb-Bioelectrode for highly selective dopamine sensing, *ACS Appl. Matter. Interfaces,* **2012**, 4, 44-48.

25. Hou, S.; Kasner, M. L.; Su, S.; Patel, K.; Cuellari, R., Highly sensitive and selective dopamine biosensor fabricated with silanized graphene, *J. Phys. Chem.,* **2010**, 114, 14915–14921.

26. Liang, W.; He, S.; Fang, J., Self-Assembly of J-Aggregate nanotubes and their applications for sensing dopamine, *Langmuir*, **2014**, 30, 805-811.

27. Nicholson, R. S.; Shain, I., Theory of Stationary Electrode Polarography. Single Scan and Cyclic Methods Applied to Reversible, Irreversible, and Kinetic Systems., *Analytical Chemistry*, **1964**, 36, 706–723.

28. Siegbahn,K.; Edvarson, K., *β-Ray spectroscopy in the precision range of 1 : 10,* Nuclear physics, 8, **1956**, 137-159.

29. Ray, S.; Shard, A. G., Quantitative Analysis of Adsorbed Proteins by X-ray Photoelectron Spectroscopy., *Analytical Chemistry*, **2011**, 83, 8659-8666.

30. White, R., Chromatography/*Fourier Transform Infrared Spectroscopy and its Applications*, CRC press, **1989**, Vol 10, 312-318.

31. Atkins, P.; de, J., *Elements of physical chemistry*, Oxford: Oxford U.P., **2009**, 5, 459.

32. Gardiner, D. J.; Graves, P. R.; Bowley, H. J., *Practical Raman spectroscopy*, New York: Springer-Verlag, **1989**, 18, 1-19.

33. Noboru, K.; Mitsuro, K.; Hiroshi, J.; Jinnai, H., Transmission electron microtomography without the 'missing wedge' for quantitative structural analysis, *Ultramicroscopy*, **2007**, 107, 8–15.

34. Wayu, M. B.; Spidle, R. T.; Devkota, T.; Deb, A. K.; Delong, R. K.; Ghosh, K. C.; Wanekaya, A. K.; Chusuei, C. C., Morphology of hydrothermally synthesized ZnO nanoparticles tethered to carbon nanotubes affects electrocatalytic activity for H_2O_2 detection, *Electrochem. Acta* **2013**, *97,* 99-104.

35. Saito, R.; Dresselhaus, G.; Dresselhaus, M. S., Physical Properties of Carbon Nanotubes, Imperial College Press: London, 1998.

36. M. Weiler, S. Sattel, K. Jung, H. Ehrhardt, V. Veerasamy, J. Robertson., Highly tetrahedral, diamond- like amorphous hydrogenated carbon prepared from a plasma beam source, *Appl. Phys. Lett.,* **1994**, *64*, 2797-2799.

37. Kanik, F. E.; Kolb, M.; Timur, S.; Bahadir, M.; Toppare, L., An amperometric acetylcholine biosensor based on a conducting polymer, *Int J Biol Macromol*, **2013**, 59, 111-118.

38. Kundu, Shankhamala, et al., Thermal stability and reducibility of oxygen-containing functional groups on multiwalled carbon nanotube surfaces: a quantitative high-resolution XPS and TPD/TPR study, *J. Phys. Chem. C,* **2008**, *112,* 16869-16878.

39. Gabriel P.; Castner, D. G.; Ratner, B. D., XPS O 1s binding energies for polymers containing hydroxyl, ether, ketone and ester groups, *Surf. Interface Anal.,* **1991**, *17*, 267-272.

40. McCafferty, E.; Wightman, J. P., Determination of the concentration of surface hydroxyl groups on metal oxide films by a quantitative XPS method, *Surf. Interface Anal.,* **1998**, *26*, 549-564.

41. Ji, L.; Lin, J.; H. C., Metal-support interactions in Co/Al_2O_3 catalysts: A comparative study on reactivity of support, *J. Phys. Chem. B*, **2000**, *104*, 1783–1790.

42. Tan, B. J.; Klabunde, K. J.; Sherwood, P. M. A., XPS studies of solvated metal atom dispersed catalysts - evidence for cobalt-manganese particles on alumina and silica, *J. Am. Chem. Soc.*, **1991**, 113, 855–861.

43. Voß, M.; Borgmann, D.; Welder, G., Characterization of alumina, silica, and titania supported cobalt catalysts, J Catal, **2002**, 212, 10–21.

44. Liu, Z. W.; Zhang, H. J.; Chen, Z. Q., Monolayer dispersion of CoO on Al_2O_3 probed by positronium atom, *Applied Surface Science,* **2014**, 293, 326– 331.

45. McPhail, M. R.; Sells, J. A.; He, Z.; Chusuei, C. C., Charging Nanowalls: Adjusting the Carbon Nanotube Isoelectric Point via Surface Functionalization, *J. Phys. Chem.,* **2009**, 113, 14102–14109.

46. Medeiros, R. A.; Lourencao, B. C.; Rocha-Filho, R. C.; Fatibello-Filho, O., Simultaneous voltammetric determination of synthetic colorants in food using a cathodically pretreated boron-doped diamond electrode, *Talanta*, **2012**, 97, 291–297.

47. Huang, J.; Liu, Y., Hou, H., You, T., Simultaneous electrochemical determination of dopamine, uric acid and ascorbic acid using palladium nanoparticle-loaded carbon nanofibers modified electrode, *Biosens. Bioelectron*, **2008**, 24, 632−637.

48. Raj, C. R.; Okajima, T.; Ohsaka, T., Gold nanoparticle arrays for the voltammetric sensing of dopamine, *J. Electroanal. Chem.*, **2003**, 543, 127−133.

49. Tian, Z. Q.; Jiang, S. P.; Liu, Z.; Li, L., Polyelectrolyte-stabilized Pt nanoparticles as new electrocatalysts for low temperature fuel cells, *Electrochem. Commun.*, **2007**, 9, 1613−1618.

50. Strawbridge, S. M.; Green, S. J.; Tucker, J. H. R., Electrochemical detection of catechol and dopamine as their phenylboronate ester derivatives, *Chem. Commun.,* **2000**, 2393-2394.

51. Fabre, B.; Taillebois, L., Poly(aniline boronic acid)-based conductimetric sensor of dopamine, *Chem. Commun.,* **2003**, 2982-2983.

APPENDIX

PERMISSION LETTERS

License Number	4357870391459
License date	May 28, 2018
Licensed Content Publisher	Elsevier
Licensed Content Publication	Materials Today
Licensed Content Title	Carbon nanotube in different shapes
Licensed Content Author	Mei Zhang,Jian Li
Licensed Content Date	Jun 1, 2009
Licensed Content Volume	12
Licensed Content Issue	6
Licensed Content Pages	7
Start Page	12
End Page	18
Type of Use	reuse in a thesis/dissertation
Portion	figures/tables/illustrations
Number of figures/tables/illustrations	1
Format	both print and electronic
Are you the author of this Elsevier article?	No
Will you be translating?	No
Original figure numbers	Fig-1
Title of your thesis/dissertation	A Cobalt Oxide Carbon Nanotube Composite for Dopamine Detection
Expected completion date	Jul 2018
Estimated size (number of pages)	80
Requestor Location	Mohammad Salauddin Kader 1245 Old Lascassas Rd Unit J MURFREESBORO, TN 37130 United States Attn: Mohammad Salauddin Kader
Publisher Tax ID	98-0397604
Total	0.00 USD

License Number	4359550785423
License date	May 31, 2018
Licensed Content Publisher	Elsevier
Licensed Content Publication	Advanced Drug Delivery Reviews
Licensed Content Title	DNA and carbon nanotubes as medicine
Licensed Content Author	William Cheung,Francesco Pontoriero,Oleh Taratula,Alex M. Chen,Huixin He
Licensed Content Date	Apr 30, 2010
Licensed Content Volume	62
Licensed Content Issue	6
Licensed Content Pages	17
Start Page	633
End Page	649
Type of Use	reuse in a thesis/dissertation
Portion	figures/tables/illustrations
Number of figures/tables/illustrations	1
Format	both print and electronic
Are you the author of this Elsevier article?	No
Will you be translating?	No
Original figure numbers	Fig: 1
Title of your thesis/dissertation	A Cobalt Oxide Carbon Nanotube Composite for Dopamine Detection
Expected completion date	Jul 2018
Estimated size (number of pages)	80
Requestor Location	Mohammad Salauddin Kader 1245 Old Lascassas Rd Unit J MURFREESBORO, TN 37130 United States Attn: Mohammad Salauddin Kader
Publisher Tax ID	98-0397604
Total	0.00 USD